Available online at www.sciencedirect.com

ScienceDirect

Geochimica et Cosmochimica Acta 179 (2016) 123–141

Geochimica et Cosmochimica Acta

www.elsevier.com/locate/gca

Clumped isotope composition of cold-water corals: A role for vital effects?

Peter T. Spooner [a,b,*], Weifu Guo [a], Laura F. Robinson [b], Nivedita Thiagarajan [c], Katharine R. Hendry [b], Brad E. Rosenheim [d,1], Melanie J. Leng [e]

[a] *Woods Hole Oceanographic Institution, Woods Hole, MA 02543, USA*
[b] *University of Bristol, Bristol BS8 1RJ, UK*
[c] *California Institute of Technology, Pasadena, CA 91125, USA*
[d] *Tulane University, New Orleans, LA 70118, USA*
[e] *British Geological Survey, Keyworth NG12 5GG, UK*

Received 8 May 2015; accepted in revised form 12 January 2016; available online 2 February 2016

Abstract

The carbonate clumped isotope thermometer is a promising tool for determining past ocean temperatures. It is based on the temperature dependence of rare isotopes 'clumping' into the same carbonate ion group in the carbonate mineral lattice. The extent of this clumping effect is independent of the isotope composition of the water from which carbonate precipitates, providing unique advantages over many other paleotemperature proxies. Existing calibrations of this thermometer in cold-water and warm-water corals suggest clumped isotope 'vital effects' are negligible in cold-water corals but may be significant in warm-water corals. Here, we test the calibration of the carbonate clumped isotope thermometer in cold-water corals with a recently collected and well characterised sample set spanning a range of coral genera (*Balanophyllia*, *Caryophyllia*, *Dasmosmilia*, *Desmophyllum*, *Enallopsammia* and *Javania*). The clumped isotope compositions (Δ_{47}) of these corals exhibit systematic dependences on their growth temperatures, confirming the basis of the carbonate clumped isotope thermometer. However, some cold-water coral genera show Δ_{47} values that are higher than the expected equilibrium values by up to 0.05‰ (equivalent to underestimating temperature by ~9 °C) similar to previous findings for some warm-water corals. This finding suggests that the vital effects affecting corals Δ_{47} are common to both warm- and cold-water corals. By comparison with models of the coral calcification process we suggest that the clumped isotope offsets in these genera are related to the kinetic isotope effects associated with CO_2 hydration/hydroxylation reactions in the corals' calcifying fluid. Our findings complicate the use of the carbonate clumped isotope thermometer in corals, but suggest that species- or genus-specific calibrations could be useful for the future application of this paleotemperature proxy.

1. INTRODUCTION

Scleractinia or 'stony corals' precipitate aragonite skeletons and range from small, solitary corals to hermatypic or 'reef-building' colonial corals that can support extremely biodiverse ecosystems. Many species living in shallow seas host photosynthesising algae, which provide the corals with carbon for metabolisation (Falkowski et al., 1984; Porter et al., 1984). Such corals are known as zooxanthellate,

* Corresponding author at: School of Earth Sciences, University of Bristol, Bristol BS8 1RJ, UK. Tel.: +44 7902008694.
E-mail address: peter.spooner@bristol.ac.uk (P.T. Spooner).
[1] Present address: University of South Florida, St. Petersburg, FL 33701, USA.

http://dx.doi.org/10.1016/j.gca.2016.01.023
0016-7037/

whereas corals that lack algal symbionts are known as azooxanthellate. Around 90% of azooxanthellate scleractinian corals live in cold/dark water and as such are often referred to as cold-water or deep-water corals (Roberts et al., 2009). The term 'cold-water coral' is also used to refer to animals from two further orders (Gorgonacea and Anthoathecata) that can have differing skeletal mineralogy. In this study we use the term 'cold-water coral' to refer specifically to azooxanthellate scleractinian corals (Roberts et al., 2006; Roberts and Cairns, 2014).

Cold-water corals are found in all major ocean basins at depths from the surface to deeper than 4000 m (Stanley and Cairns, 1988; Roberts et al., 2006; Cairns, 2007). Their skeletons can be collected from the seafloor and precisely dated using uranium-series techniques (Cheng et al., 2000). As such, they are a promising target as an archive of past ocean dynamics and properties, particularly for regions lacking sediment-core climate records (Robinson et al., 2014).

Given the important role of temperature in governing seawater density, circulation and heat transport, numerous geochemical proxy-methods have been developed and applied to reconstruct past ocean temperature (eg. McCrea, 1950; Alibert and McCulloch, 1997; Barker et al., 2005; Rueggeberg et al., 2008; Thiagarajan et al., 2014). However, many paleotemperature proxies used successfully in other archives (eg. $\delta^{18}O$ and Mg/Ca in foraminiferal tests) cannot be straightforwardly applied in cold-water corals (eg. Smith et al., 2000; Adkins et al., 2003; Gagnon et al., 2007; Case et al., 2010). This complication is due to the presence of 'vital effects', i.e. biological processes that cause deviations of coral geochemical compositions from thermodynamic equilibrium values. For example, the stable isotope compositions ($\delta^{18}O$ and $\delta^{13}C$) of cold-water coral skeletons are known to be depleted relative to the expected carbonate-seawater equilibrium values by up to 6–12‰ (Adkins et al., 2003; Lopez Correa et al., 2010; Lutringer et al., 2005; Mortensen and Rapp, 1998; Smith et al., 2000; Spiro et al., 2000; Rollion-Bard et al., 2003, 2010; Marali et al., 2013). The magnitude of these stable isotope vital effects varies even within a coral skeleton and is thought to be related to kinetic and/or pH-driven processes during coral calcification (eg. McConnaughey, 1989; Adkins et al., 2003). A proxy that is neither affected by biological mediation nor requires knowledge of the seawater isotopic composition would be a valuable tool for the paleoceanographic community.

A promising paleotemperature proxy in this regard is the clumped isotope composition of coral skeletal carbonate (Ghosh et al., 2006; Thiagarajan et al., 2011; Saenger et al., 2012). It is based on the homogeneous isotope equilibrium within the carbonate lattice, and thus can constrain carbonate formation temperature without knowledge of the isotopic composition of the water from which the carbonate grew. An example of such an isotope equilibrium is:

$$Ca^{13}C^{16}O_3 + Ca^{12}C^{18}O^{16}O_2 \Longleftrightarrow Ca^{13}C^{18}O^{16}O_2 + Ca^{12}C^{16}O_3$$

Under thermodynamic equilibrium, ^{13}C and ^{18}O in the carbonate lattice have a tendency to clump into the same carbonate ion group, leading to a relative enrichment in the abundance of the $^{13}C^{18}O^{16}O_2^{2-}$ isotopologue over that which would be expected if all isotopes were randomly distributed. The magnitude of this enrichment varies as a function of the carbonate formation temperature and can thus be used as a geothermometer.

In practice this enrichment is quantified by measuring the abundance anomalies of the mass 47 isotopologues (mostly $^{13}C^{18}O^{16}O$) in CO_2 derived from phosphoric acid digestion of carbonates, which is proportional to the enrichment of the $^{13}C^{18}O^{16}O_2^{2-}$ isotopologue in the carbonate mineral (Ghosh et al., 2006; Guo et al., 2009b):

$$\Delta_{47} = \left[\left(\frac{R_{47}}{R^*_{47}} - 1\right) - \left(\frac{R_{46}}{R^*_{46}} - 1\right) - \left(\frac{R_{45}}{R^*_{45}} - 1\right)\right] \times 1000,$$

where R_{47}, R_{46}, and R_{45} are the measured abundance ratios of masses 47, 46 and 45 relative to mass 44, and the denominator terms R^* are the expected ratios if all isotopes were randomly distributed (i.e. if the sample had the stochastic distribution of isotopologues based on its measured $\delta^{18}O$ and $\delta^{13}C$ values) (Eiler and Schauble, 2004; Huntington et al., 2009).

Ghosh et al. (2006) first calibrated the carbonate clumped isotope thermometer by precipitating synthetic calcites in the lab, yielding a temperature relationship of $\Delta_{47} = 0.0592 \times 10^6/T^2 - 0.02$ (T in kelvin). Subsequently, Dennis and Schrag (2010) precipitated calcites and found a Δ_{47} temperature dependence of $\Delta_{47} = 0.0337 \times 10^6/T^2 + 0.247$, significantly different from that of Ghosh et al. (2006). We refer to these contrasting calibrations as the Ghosh calibration line and the Dennis calibration line throughout this study. The discrepancies between these calibration lines are not resolved by converting the measured Δ_{47} values to the absolute reference frame (ARF) (Dennis et al., 2011). Recently Zaarur et al. (2013) repeated similar precipitation experiments to Ghosh et al. (2006) and found a temperature dependence close to the Ghosh calibration line for calcite and aragonite. In contrast, weaker temperature dependences of the clumped isotope thermometer in aragonite similar to the Dennis calibration line have also since been reported (Kim et al., 2010; Defliese et al., 2015). The causes of the different calibration slopes – which also exist in the calibration of some biogenic carbonates, e.g. brachiopods (Henkes et al., 2013; Came et al., 2014; Petrizzo et al., 2014) – are a matter of current debate within the clumped isotope community. It has been postulated that these inter-laboratory differences are related to differences in the analytical protocols in different labs, e.g. the extent of equilibration between the produced CO_2 and the water associated with the digestion acid (Came et al., 2014; Defliese et al., 2015).

Despite the complications described above, calibrations of the clumped isotope thermometer in many (although not all) biogenic carbonates appear to agree closely with the Ghosh calibration line (Came et al., 2007; Tripati et al., 2010; Thiagarajan et al., 2011; Zaarur et al., 2011; Eagle et al., 2013). However, with the exception of Eagle et al. (2013), these studies used the same analytical methods as Ghosh et al. (2006). Confidence in the application of the carbonate clumped isotope thermometer in cold-water corals increased with the finding that the relationship between

their clumped isotope compositions and growth temperature was indistinguishable from the Ghosh calibration line (Thiagarajan et al., 2011). This result highlighted the possibility that the processes generating large vital effects in coral $\delta^{18}O$ and $\delta^{13}C$ did not affect clumped isotope fractionations in cold-water corals. The carbonate clumped isotope thermometer has since then been applied to the cold-water coral *Desmophyllum dianthus*, to explore past ocean temperatures (Thiagarajan et al., 2014). In contrast, the clumped isotope compositions of some warm-water scleractinian corals were shown to be systematically offset from the Ghosh calibration line by ~0.04‰ (Saenger et al., 2012). Such clumped isotope vital effects in warm-water corals did not seem to be related to the presence or absence of algal symbionts (Saenger et al., 2012). In this study we increase the sample density of the calibration of the clumped isotope thermometer in cold-water corals with a new, recently-collected and well- characterised sample set spanning a range of coral genera. We test and correct for inter-laboratory differences in clumped isotope measurements, allowing direct comparison of our results with results from previous studies, and we further evaluate the possible causes of clumped isotope vital effects in scleractinian corals.

2. MATERIALS AND METHODS

2.1. Coral samples

Corals analysed in this study were either collected during recent cruises to the Atlantic and Southern Oceans (Table S1), or have been measured before (Thiagarajan et al., 2011). Samples from the tropical Atlantic Ocean were collected during the JC094 cruise (Oct–Nov 2013, Robinson, 2014) by Remote Operated Vehicle (ROV) from the flanks of seamounts or fracture zone escarpments, with the depth of collection ranging from 200 m to 2500 m. These samples were all living immediately prior to collection. Coral samples from the Southern Ocean were collected during three cruises to the Drake Passage (NBP-0805, NBP-1103 and LMG-0605) (Burke et al., 2010; Margolin et al., 2014). These samples were collected using dredge or trawl deployments, on the flanks of seamounts, fracture zones and the continental margin between 330 m and 1879 m. The corals were not alive when collected, but were determined to be less than 1000 years old using uranium-series and/or reconnaissance radiocarbon dating (Burke and Robinson, 2012; Margolin et al., 2014). If necessary, coral samples were bleached and then rinsed with fresh water while on board ship to remove organic tissue and were stored at room temperature.

We analysed a total of six genera of corals from these recent collections, with four of them from the Atlantic Ocean collection: *Caryophyllia* (solitary); *Dasmosmilia* (solitary); *Enallopsammia* (colonial); *Javania* (solitary), and two from the Southern Ocean collection: *Balanophyllia* (solitary) and *Desmophyllum* (solitary) (Tables 1, S1). We also analysed new subsamples from five coral specimens previously measured by Thiagarajan et al. (2011) (Tables 1, S1).

2.2. Seawater properties

2.2.1. Temperature

Temperature estimates at each sample site were derived from at least two (up to three) different sources: (1) annual average temperature data from the Levitus94 (Levitus and Boyer, 1994) database from within 0.5° latitude and longitude, and extrapolated to the depth of sample collection; (2) ROV CTD data at the sample collection site (JC094 cruise only, including the maximum and minimum ROV CTD temperature recorded within ±3 m depth of the collection site) and (3) rosette CTD data taken near the sample site and extrapolated to the depth of sample collection (in some cases two rosette casts were available from different cruises). For most cases, data from the available sources agreed to within ±0.4 °C and we take this to be the uncertainty on our estimates of coral growth temperature (Table S1). The exceptions were for samples JC094-B0457-Daslm-001 and JC094-B0468-Daslm-001 collected from within the Atlantic thermocline. The rosette CTD measured temperatures were 1 °C and 2 °C warmer than those measured using the ROV for the two samples respectively, while the Levitus94 temperatures agreed with the ROV data to within 0.2 °C. The differing temperature estimates here are likely due to changes in the thermocline depth with proximity to the seamount and/or diurnal changes. It is also possible that seasonal variation in the thermocline is important for this site. This uncertainty does not alter our conclusions. In all figures and tables we report the temperatures measured by the CTD mounted on the ROV or rosettes.

2.2.2. Carbon and oxygen isotopic compositions of seawater

The isotopic compositions of seawater were determined based on waters collected in Niskin bottles during all cruises, which were attached to either the rosette system (12 collections per deployment) or the ROV (JC094 cruise only, up to 5 collections per deployment).

For $\delta^{13}C$ measurements, unfiltered seawater samples were collected in 250 ml acid-cleaned and ashed glass bottles from the Niskin bottles using acid-cleaned silicone tubing, first rinsing and then overfilling the bottle by at least 50%. The sample, leaving head-space, was poisoned with 50 µl of saturated mercuric chloride solution, and the bottle was then sealed with a plastic screwcap lid and o-ring. The $\delta^{13}C$ of dissolved inorganic carbon (DIC, 1 standard deviation S.D. = 0.1‰) was analysed at the University of California (Irvine) for tropical Atlantic samples (Gao et al., 2014), and at the National Ocean Sciences Accelerator Mass Spectrometry facility (NOSAMS) of Woods Hole Oceanographic Institution for Southern Ocean samples. The speciation of DIC in the seawater was calculated based on the seawater alkalinity and total DIC concentration estimated from the GLODAP database and measured temperatures, using the CO2SYS program (van Heuven et al., 2011). The $\delta^{13}C$ of the dissolved HCO_3^- was then calculated based on the measured $\delta^{13}C_{DIC}$ and published carbon isotope fractionation factors (Mook et al., 1974). The calculated $\delta^{13}C_{HCO_3^-}$ is typically 0.1–0.2‰ greater than the

Table 1
Stable isotope compositions of seawater and cold-water coral samples analysed in this study.

Sample info.	Seawater properties			Sample isotope data						
Sample label and genus	T (°C)	$\delta^{18}O$ VSMOW (‰)	$\delta^{13}C$ VPDB HCO_3^- (‰)	n	Δ_{47} (‰)	Err. (‰)	$\delta^{18}O$ VPDB (‰)	Err. (‰)	$\delta^{13}C$ VPDB (‰)	Err. (‰)
NBP1103-DH07-Bc-02 (**B**)	4.8	−0.76	1.59	3	0.862	0.002	1.50	0.02	−4.57	0.04
NBP1103-DH14-Bn-282 (**B**)	3.9	−0.66	1.21	3	0.866	0.010	1.13	0.02	−6.15	0.06
NBP1103-DH16-Bn-11 (**B**)	2.6	−0.52	0.76	3	0.875	0.010	2.12	0.02	−5.33	0.01
LMG06-05-3-2 (**B**)	5.2	−0.57	1.65	3	0.857	0.021	1.18	0.02	−5.49	0.08
49020 (**C**)	17.4	0.91	–	4	0.773	0.011	1.64	0.01	0.17	0.01
JC094-B0040-Carlm-001 (**C**)	3.0	0.23	1.14	8	0.823	0.003	3.82	0.01	−0.09	0.04
JC094-B0244-Carls-001 (**C**)	7.9	0.18	0.61	8	0.814	0.005	2.39	0.04	−2.19	0.05
JC094-B0561-Carlm-001 (**C**)	4.3	0.24	0.56	8	0.806	0.003	3.41	0.04	−0.93	0.15
JC094-B0579-Carlm-001 (**C**)	4.4	0.24	0.56	5	0.145	0.013	2.99	0.23	−1.46	0.40
JC094-B0579-Carlm-002 (**C**)	4.4	0.24	0.56	5	0.818	0.011	3.73	0.02	0.16	0.02
JC094-B0597-Carls-001 (**C**)	6.1	0.11	0.6	8	0.819	0.007	2.68	0.01	−2.27	0.01
JC094-B2242-Carlm-001 (**C**)	4.4	0.26	0.84	19	0.800	0.005	4.09	0.02	1.38	0.02
JC094-B0457-Daslm-001 (**Da**)	10.6	0.35	0.37	8	0.815	0.005	−0.52	0.02	−8.37	0.02
JC094-B0468-Daslm-001 (**Da**)	12.2	0.40	0.35	8	0.798	0.005	0.14	0.02	−5.85	0.02
47413 (**De**)	7.9	−0.44	–	4	0.802	0.006	0.80	0.01	−5.49	0.03
80404 (**De**)	13.1	0.25	–	4	0.797	0.003	0.14	0.02	−6.24	0.03
NBP1103-DH22-Dc(f)6 (**De**)	2.3	−0.57	0.65	3	0.833	0.010	2.90	0.05	−2.71	0.08
NBP1103-DH97-Dp-1 (**De**)	2.7	−0.47	0.89	3	0.821	0.010	2.61	0.03	−3.64	0.05
NBP0805-TB04-DpA-003 (**De**)	3.7	−0.66	1.21	3	0.820	0.004	1.42	0.03	−5.73	0.06
NBP1103-TB10-Dp-1 (**De**)	3.9	−0.66	1.21	3	0.832	0.006	1.57	0.02	−4.97	0.04
JC094-B0141-Enall-001 (**E**)	4.3	0.24	0.56	6	0.842	0.004	0.89	0.05	−5.06	0.03
JC094-B1030-Enall-001 (**E**)	7.3	0.14	0.89	4	0.837	0.011	2.47	0.02	−1.52	0.03
JC094-B1054-Enall-001 (**E**)	3.7	0.26	1.14	4	0.846	0.009	2.84	0.04	−1.69	0.09
47531 (**E**)	7.5	−0.14	–	4	0.832	0.004	1.28	0.001	−2.22	0.03
77019 (**E**)	14.3	0.95	–	4	0.806	0.005	1.13	0.03	−6.01	0.03
JC094-B0023JaA-lm-001 (**J**)	4.4	0.24	0.56	5	0.815	0.005	3.79	0.02	0.09	0.02
JC094-B0030-JaCls-001 (**J**)	3.1	0.23	1.14	3	0.805	0.007	4.02	0.03	0.31	0.09
JC094-B0561-JaClm-001 (**J**)	4.3	0.24	0.56	8	0.834	0.006	2.83	0.02	−1.38	0.04
JC094-B2245-JaClm-001 (**J**)	5.5	0.20	1.16	4	0.827	0.002	2.98	0.03	−1.06	0.01
JC094-B1866-Javls-001 (**J**)	4.4	0.25	0.95	4	0.826	0.006	3.65	0.03	0.24	0.01
JC094-B2067-Javls(f)-001 (**J**)	7.4	0.20	0.79	4	0.821	0.003	3.34	0.01	0.33	0.03
JC094-B2095-Javlm-001 (**J**)	6.0	0.12	0.89	4	0.817	0.005	3.24	0.005	−0.23	0.05

Genera are labelled according to the following abbreviations: *Balanophyllia* (B), *Caryophyllia* (C), *Dasmosmilia* (Da), *Desmophyllum* (De), *Enallopsammia* (E) and *Javania* (J). *n* indicates the number of replicate measurements for each sample, excluding cleaned aliquots. Data presented are the averages of all measurements for each coral which in some cases are from more than one subsample (i.e. theca and septa), excluding cleaned aliquots. Corals 49,020, 47,413, 80,404, 47,531 and 77,019 were also measured by Thiagarajan et al. (2011). Errors are ±1 S.E.

corresponding $\delta^{13}C_{DIC}$. All $\delta^{13}C$ values are reported relative to Vienna Pee-Dee Belemnite (VPDB).

For $\delta^{18}O$ measurements, unfiltered 60 ml subsamples were sealed using rubber stoppers and aluminium crimp seals in glass bottles and stored in cool (~4 °C), dark conditions for transportation. For the tropical Atlantic samples, the $\delta^{18}O$ measurements were conducted using the IsoPrime100 with Aquaprep system at the NERC Isotope Geosciences Laboratory, with typical precisions of ±0.02‰ (1 S.D.). For Southern Ocean samples, the $\delta^{18}O$ measurements were conducted using the Isoprime Multiprep system at Tulane University, with precisions of ±0.24‰ (1 S.D.). In the tropical Atlantic, measurements of $\delta^{18}O$ had poorer spatial coverage than measurements of $\delta^{13}C$. We therefore elected to calculate the ocean atlas-derived seawater $\delta^{18}O$ for sample sites from this cruise, following the methods in Thiagarajan et al. (2011). A regional relationship between $\delta^{18}O$ and salinity was established using the NASA Global Seawater Oxygen-18 Database – v1.21 (Schmidt et al., 1999). The more finely gridded Levitus94 salinity database was then used to estimate $\delta^{18}O$ near the sample site. Where possible, the calculated $\delta^{18}O$ values were compared with the values derived from measurements of water samples at the respective sites. The maximum offset between the ocean atlas estimate and in-situ measured $\delta^{18}O$ was 0.1‰, about equal to the error on the ocean atlas estimate (Thiagarajan et al., 2011) and small compared to the range of $\delta^{18}O$ variability we observed amongst different corals (~4‰). Such small uncertainties in seawater $\delta^{18}O$ shall not affect our conclusions. The $\delta^{18}O$ of the seawater samples are reported relative to Vienna Standard Mean Ocean Water (VSMOW).

2.3. Stable isotope measurements of coral skeletons

The surfaces of each coral sample were scraped with a dremel tool to remove residual organic material (Thiagarajan et al., 2011). Aliquots of approximately 30 mg were cut from each specimen with a diamond blade, rinsed with 18 MΩ cm water and ground to powders/fine grains with a pestle and mortar. For seven solitary corals, subsamples were taken from both the theca and septa of the skeleton to assess any systematic differences in the clumped isotope composition between these two important skeletal architectures (Table 2). We also carried out an experiment on NBS-19 and two coral samples to evaluate the impact of oxidative cleaning on the measured Δ_{47} (Table 3). For this experiment, crushed samples were subjected to water rinses, a 15 min wash in 30% H_2O_2 + 1 M NaOH (mixed in the ratio 1:1) at 40 °C, and a rinse lasting 1–2 min in (0.1 M) perchloric acid, similar to methods designed to vigorously remove organic material in preparation for uranium-series dating of cold-water coral skeletons (Cheng et al., 2000). Both cleaned and uncleaned powders of these samples were analysed. Except for samples employed in this experiment, all other samples in this study were not chemically cleaned prior to analysis, consistent with the procedure of previous clumped isotope studies of corals (Thiagarajan et al., 2011; Saenger et al., 2012).

Multiple aliquots (~4 mg each) of each coral sample were weighed into silver capsules and added to an autosampler in a random order. This randomising procedure was used in order to reduce the possibility of systematic instrumental effects affecting repeat measurements of a single sample. Each aliquot of a single powdered sample was generally analysed within a single measurement session, over the course of 3–4 days. An aliquot of one of two in-house carbonate standards (NBS-19 or 102-GC-AZ01) was analysed after every ~7 coral aliquots. Between 3 and 5 aliquots were analysed for the majority of coral subsamples, resulting in 8 or more replicate measurements of many coral specimens (where the theca and septa of the same specimen were sampled).

Clumped isotope analyses were performed at Woods Hole Oceanographic Institution (WHOI), within two measurement sessions (May–July 2014 and September 2014), on a Thermo Scientific MAT-253 mass spectrometer coupled to a custom-built automated acid reaction and gas purification line. The purification line is similar to the one described by Henkes et al. (2013), except both heated gases and equilibrated gases were introduced by first freezing them in liquid nitrogen (LN_2) as opposed to directly injecting them into a helium stream.

Aliquots of carbonate samples and standards were digested in 103% H_3PO_4 ($\rho = 1.92$ g/cm^3) at 90 °C and evolved CO_2 was purified by passing through several cryogenic traps (−78 °C dry ice/ethanol slush, and liquid nitrogen trap) and a custom-built packed 60 cm-long gas chromatograph column (Porapak Q, 50–80 mesh) held at −20 °C. Purified CO_2 gases were then expanded into the sample bellow of the mass spectrometer and analysed at a bellow gas pressure corresponding to a signal of 12 V on the Faraday cup measuring mass 44 of CO_2. A bottle of Oztech CO_2 ($\delta^{13}C_{VPDB} = -3.63$‰, $\delta^{18}O_{VSMOW} = +25.04$‰) was used as the working reference gas during isotope measurements. Each measurement sequence consisted of six acquisitions, and each acquisition consisted of 9 cycles of sample-reference comparison with 20 or 26 s of integration time.

The $\delta^{18}O$ and $\delta^{13}C$ values of carbonates were calculated using the working reference gas and then normalised by reference to the NBS-19 standard analysed in the same measurement session. CO_2 gases equilibrated at 1000 °C and 25 °C (i.e. 'heated gases' and 'equilibrated gases') were processed using the same purification line and analysed regularly to convert all clumped isotope values to the absolute reference frame (Dennis et al., 2011). An acid digestion fractionation of 0.092‰ was applied to normalise the clumped isotope composition of all carbonate standards and samples to acid extractions at 25 °C (Henkes et al., 2013). The analytical precision of each measurement session was ±0.016‰, ±0.13‰ and ±0.06‰ (1 S.D.) for Δ_{47}, $\delta^{18}O$ and $\delta^{13}C$ respectively, based on repeated measurements of the two in-house carbonate standards. Where n subsamples of a coral were measured, standard errors (1 S.E.) on isotope ratios were calculated by dividing the 1 S.D. of those measurements by $\sqrt{n}$.

In addition to isotope measurements made at WHOI, homogenised powders of five coral specimens were shared

Table 2
Stable isotope compositions of separate subsamples taken from individual coral specimens (eg. septa or theca).

Sample info.		Sample isotope data						
Sample label and genus	Skeletal region	*n*	Δ_{47} (‰)	Err. (‰)	δ^{18}O VPDB (‰)	Err. (‰)	δ^{13}C VPDB (‰)	Err. (‰)
JC094-B0040-Carlm-001 (s1) (**C**)	Septa	5	0.822	0.003	3.99	0.01	0.47	0.02
JC094-B0040-Carlm-001 (th1) (**C**)	Theca	3	0.826	0.008	3.54	0.01	−1.01	0.07
JC094-B0244-Carls-001 (s1) (**C**)	Septa	5	0.811	0.008	2.58	0.04	−1.67	0.07
JC094-B0244-Carls-001 (th1) (**C**)	Theca	3	0.820	0.003	2.08	0.08	−3.05	0.07
JC094-B0597-Carls-001 (s1) (**C**)	Septa	5	0.823	0.011	2.60	0.01	−2.42	0.02
JC094-B0597-Carls-001 (th1) (**C**)	Theca	3	0.812	0.012	2.81	0.02	−2.03	0.02
JC094-B2242-Carlm-001 (s1) (**C**)	Septa	7	0.786	0.006	4.20	0.03	1.89	0.05
JC094-B2242-Carlm-001 (th1) (**C**)	Theca	8	0.800	0.005	4.00	0.02	1.03	0.02
JC094-B2242-Carlm-001 (b) (**C**)	Mix	4	0.825	0.009	4.08	0.03	1.17	0.01
JC094-B0457-Daslm-001 (s1) (**Da**)	Septa	5	0.812	0.009	−0.85	0.02	−9.07	0.01
JC094-B0457-Daslm-001 (th1) (**Da**)	Theca	3	0.821	0.003	0.01	0.03	−7.20	0.03
JC094-B0468-Daslm-001 (s1) (**Da**)	Septa	5	0.802	0.008	0.67	0.03	−4.52	0.03
JC094-B0468-Daslm-001 (th1) (**Da**)	Theca	3	0.792	0.005	−0.74	0.01	−8.08	0.03
JC094-B0141-Enall-001 (1) (**E**)	Mix	5	0.839	0.005	0.78	0.03	−5.21	0.02
JC094-B0141-Enall-001 (2) (**E**)	Mix	1	0.855	0.016	1.45	0.09	−4.32	0.05
JC094-B0561-JaClm-001 (s1) (**J**)	Septa	5	0.827	0.007	3.18	0.01	−0.51	0.02
JC094-B0561-JaClm-001 (th1) (**J**)	Theca	3	0.846	0.011	2.25	0.03	−2.82	0.08

Genera are labelled according to the following abbreviations: *Balanophyllia* (B), *Caryophyllia* (C), *Dasmosmilia* (Da), *Desmophyllum* (De), *Enallopsammia* (E) and *Javania* (J). *n* indicates the number of replicate measurements for each subsample, excluding cleaned aliquots. Errors are ±1 S.E.

Table 3
Effects of oxidative cleaning on the measured clumped isotope composition of carbonates.

Cleaning protocol	Sample	Δ_{47} (‰)			References
		Uncleaned	Cleaned	Diff.	
15 min 1:1 NaOH (1 M) + H_2O_2 (30%), followed by 1–2 min $HClO_4$ (0.1 M)	NBS-19	0.442 ± 0.004	0.430 ± 0.003	−0.012	This study
	JC094-B0561-JaClm-001(th1)	0.846 ± 0.010	0.830 ± 0.006	−0.016	
	JC094-B0561-Carlm-001	0.813 ± 0.005	0.815 ± 0.004	0.002	
30 min H_2O_2 (3%)	JR-126	0.716 ± 0.005	0.716 ± 0.012	0.000	Eagle et al. (2013)
	JR-131	0.714 ± 0.005	0.709 ± 0.002	−0.005	
4 h H_2O_2 (10%)	RIB-B54	0.732 ± 0.011	0.750 ± 0.015	0.018	Saenger et al. (2012)

Δ_{47} values are reported in the absolute reference frame. ±Values are 1 S.E.

between WHOI and the California Institute of Technology (Caltech) to evaluate potential inter-laboratory differences in clumped isotope measurements. These samples were from four different coral genera (Table 4).

2.4. Processing of coral clumped isotope data from previous studies

Clumped isotope compositions of coral skeletons have been reported in previous studies, e.g. Thiagarajan et al. (2011) and Saenger et al. (2012). Saenger et al. (2012) presented their data in the ARF based on a secondary transfer function constructed from three in-house standards (a Carrara marble, corn CO_2, and CO_2 equilibrated with water at 25 °C). The data from Thiagarajan et al. (2011) were not originally reported in the ARF. Previous attempts to convert the Thiagarajan et al. (2011) data were based on measurements of heated gases and NBS-19 made around the time of the study, and used the 'tertiary reference frame' approach in Dennis et al. (2011), also often used to convert the original Ghosh et al. (2006) data (Dennis et al., 2011; Saenger et al., 2012; Eagle et al., 2013).

Recently, four of the corals measured in Thiagarajan et al. (2011) have been re-sampled and analysed at Caltech in the ARF. Together with another cold-water coral that has previously been measured in the ARF (Dennis et al., 2011), these data enable us to provide an updated conversion of the Thiagarajan et al. (2011) data to the ARF. Our approach is the same as the 'tertiary reference frame' approach above, with the exception that we use the re-analysed corals as additional carbonate standards to better-constrain the conversion. In addition, rather than a single conversion for data generated during multiple sessions, we use a session-by-session conversion for each of the seven sessions in 2008 in which cold-water corals were measured for Thiagarajan et al. (2011). For each session, we constructed an empirical transfer function based on the known ARF Δ_{47} values for heated gases, NBS-19 and/or re-analysed corals run during that session. If a coral was not re-analysed in the ARF, this function was used to convert the clumped isotope data reported in Thiagarajan et al. (2011) to the ARF. For corals that were re-analysed in the ARF, we use the measured ARF value. The updated coral data, including the standards/corals used for the conversions, are presented in Table S4.

3. RESULTS

3.1. Oxygen and carbon isotope compositions

Coral $\delta^{18}O_{VPDB}$ ranged from −0.85‰ to 4.2‰, and $\delta^{13}C_{VPDB}$ ranged from −9.07‰ to 1.89‰ (sample averages, Tables 1 and 2). The coral genera *Caryophyllia* and *Javania* typically contained the most enriched isotopic compositions ($\delta^{18}O_{VPDB}$ ~2‰ to 4‰, $\delta^{13}C_{VPDB}$ ~ −3‰ to 2‰) and the genus *Dasmosmilia* contained the most depleted compositions ($\delta^{18}O_{VPDB}$ ~ −1‰ to 1‰, $\delta^{13}C_{VPDB}$ ~ −9‰ to −4‰). The maximum difference in $\delta^{18}O_{VPDB}$ between two subsamples of a single specimen was 1.5‰ in the coral JC094-B0468-Daslm-001 (*Dasmosmilia* sp.), accompanied by a difference in $\delta^{13}C_{VPDB}$ of 3.5‰. Differences within other coral specimens ranged from 0.2‰ to 1‰ for $\delta^{18}O_{VPDB}$ and 0.4‰ to 2.5‰ for $\delta^{13}C_{VPDB}$.

For each coral analysed, we estimated the expected $\delta^{18}O$ and $\delta^{13}C$ values if they had formed in isotope equilibrium with seawater, based on seawater data for the sample site (T, $\delta^{18}O_{sw}$, $\delta^{13}C_{HCO_3^-}$) and published equilibrium isotope fractionation factors (Grossman and Ku, 1986; Romanek et al., 1992). The $\delta^{18}O$ and $\delta^{13}C$ of the majority of samples were depleted with respect to the expected equilibrium values, consistent with findings from previous studies (Fig. 1, Table 1, Table S1) (Adkins et al., 2003; Lutringer et al., 2005; Mortensen and Rapp, 1998; Smith et al., 2000; Rollion-Bard et al., 2003, 2010). Oxygen and carbon isotope depletions (i.e. $\Delta\delta^{18}O$ and $\Delta\delta^{13}C$) are known to be linearly correlated across most parts of a cold-water coral skeleton, with $\Delta\delta^{13}C/\Delta\delta^{18}O$ slopes typically around 2.3 and intercepts ranging from −5‰ to −1‰ (Adkins et al., 2003; Lutringer et al., 2005; Mortensen and Rapp, 1998; Smith et al., 2000; Rollion-Bard et al., 2003, 2010). The isotopic compositions of corals measured in this study fall within the region covered by these previously-determined slopes and intercepts, with the magnitude of the disequilibrium effects varying amongst different coral genera (Fig. 1). For example, the majority of data for the genera *Caryophyllia* and *Javania* fall within 1‰ of the expected equilibrium $\delta^{18}O$ values, whereas the majority of data for *Balanophyllia*, *Dasmosmilia* and *Enallopsammia* are more than 1‰ from the expected equilibrium values, with the species *D. dianthus* straddling these two extremes. However, previous micro-sampling measurements of *Caryophyllia*

and *Desmophyllum* corals show that both genera can contain the entire range of isotopic depletion observed for cold-water corals (Smith et al., 2000; Adkins et al., 2003). It therefore seems probable that the differences we observe between genera are due to sampling biases, rather than the true extent of $\delta^{18}O$ and $\delta^{13}C$ disequilibrium.

3.2. Clumped isotope compositions

3.2.1. Effect of oxidative cleaning

We compared measurements of both cleaned and uncleaned powders from one carbonate standard (NBS-19) and two coral samples (Table 3). Each powder was measured 3 times, with the exception of the uncleaned NBS-19, which was measured 12 times. The maximum difference in Δ_{47} between cleaned and uncleaned powders was 0.016‰ for the coral JC094-B0561-JaClm-001 (*Javania*) and the minimum was 0.002‰ for the coral JC094-B0561-Carlm-001 (*Caryophyllia*). T-tests indicated that there was no significant difference between the Δ_{47} of cleaned and uncleaned powders for any of the samples ($p = 0.10$ for NBS-19, $p = 0.20$ for JC094-B0561-JaClm-001 and $p = 0.63$ for JC094-B0561-Carlm-001). Two previous studies of biogenic aragonites, employing only H_2O_2 treatment, also indicated that oxidative cleaning does not have a statistically significant effect on measured Δ_{47} values (Table 3, Saenger et al., 2012; Eagle et al., 2013). Therefore coral samples in this study were not cleaned prior to isotope analysis with the exception of shipboard bleaching, water rinses and physical scraping, consistent with the procedure of Thiagarajan et al. (2011) and Saenger et al. (2012).

3.2.2. Inter-laboratory comparison

Measurements of two carbonate standards at WHOI (NBS19 and 102-GC-AZ01) yielded consistent Δ_{47} values between the two measurement sessions, with averages of 0.438 ± 0.011‰ (1 S.D., $n = 12$) and 0.749 ± 0.016‰ ($n = 13$) during the first measurement session (May–July, 2014), and 0.432 ± 0.023‰ ($n = 10$) and 0.740 ± 0.013‰ ($n = 9$) during the second measurement session (September, 2014). These values are however systematically higher than the mean values reported in recent studies, i.e. 0.392 ± 0.017‰ and 0.713 ± 0.012‰ for NBS-19 (a Carrara marble) and 102-GC-AZ01 respectively (Dennis et al., 2011; Zaarur et al., 2013).

The magnitudes of our observed offsets (0.027–0.046‰) relative to the mean values reported in previous studies are close to the range of inter-laboratory difference observed in previous studies, which are up to 0.031‰ for NBS19 (0.057‰ for Carrara marble) and 0.023‰ for 102-GC-AZ01 (Dennis et al., 2011; Rosenheim et al., 2013; Zaarur et al., 2013; Tang et al., 2014). The exact cause of these offsets could be related to the differences in our analytical procedure and/or the phosphoric acid digestion fractionation factor (0.092‰) we adopted, and warrants further investigation. In this study, we corrected our clumped isotope data based on the linear function required to bring the values of these in-house standards measured at WHOI into agreement with their previously reported values (see details below). This linear function is a Δ_{47}-dependent empirical transfer function, equivalent to that described in Dennis et al. (2011), but applied after the 'heated gas', 'equilibrated gas' and acid digestion corrections that transfer data into the ARF. Therefore, this additional correction means that our reported clumped isotope data are no longer strictly in the ARF.

Note that the clumped isotope value of the 102-GC-AZ01 standard reported by the Caltech laboratory in Dennis et al. (2011) was greater than the inter-lab average value (0.724‰ vs. 0.713‰). We therefore corrected our inter-laboratory comparison dataset in two ways, by assuming two different values for the 102-GC-AZ01

Table 4
Results of the inter-laboratory comparison of clumped isotope measurements between WHOI and Caltech.

Sample info.	Sample isotope data				
Sample label	Measurement	*n*	Δ_{47} (‰)	Err. (‰)	Offset from Caltech value
NBP1103-DH14-Bn-282	WHOI[1]	3	0.850	0.009	−0.016
	WHOI[2]	3	0.866	0.010	0.000
	Caltech	5	0.866	0.009	–
LMG06-05-3-2	WHOI[1]	3	0.841	0.020	−0.010
	WHOI[2]	3	0.857	0.021	0.006
	Caltech	4	0.851	0.007	–
JC094-B2242-Carlm-001 (b)	WHOI[1]	4	0.0811	0.008	−0.011
	WHOI[2]	4	0.825	0.009	0.003
	Caltech	4	0.822	0.004	–
NBP1103-DH97-Dp-1	WHOI[1]	3	0.806	0.009	−0.023
	WHOI[2]	3	0.821	0.010	−0.008
	Caltech	5	0.829	0.008	–
JC094-B1054-Enall-001	WHOI[1]	4	0.831	0.009	−0.001
	WHOI[2]	4	0.846	0.009	0.014
	Caltech	5	0.832	0.005	–

Measurements were made on aliquots of the same coral powders. Δ_{47} values from the Caltech lab are reported in the absolute reference frame of Dennis et al. (2011). Δ_{47} values from the WHOI lab are corrected based on linear functions required to bring the values of the carbonate standards into agreement with either the inter-lab average value (0.713‰) for 102-GC-AZ01 (WHOI[1]) or with the Caltech value (0.724‰, WHOI[2]) reported in Dennis et al. (2011). Errors are ±1 S.E. See details in Section 3.2.2.

standard, i.e. 0.713‰ and 0.724‰. We evaluated the robustness of these corrections based on comparisons with measurements made at both WHOI and Caltech on five homogenised coral powders (Section 2.3.).

Excellent agreement was observed between the WHOI and Caltech measurements of these five coral powders, when we corrected our data using the 0.724‰ value for 102-GC-AZ01, i.e. the value specifically from the Caltech laboratory (Dennis et al., 2011) (Fig. 2, Table 4). Such agreement highlights the usefulness of using carbonate standards to remove inter-lab bias, which can exist despite converting all measurements into the ARF. Given these results, and our aim of comparing our values with previous measurements made at Caltech (Thiagarajan et al., 2011), all data measured at WHOI presented in this study were corrected using the 0.724‰ value for 102-GC-AZ01 (Table S2). Data corrected using the inter-lab average value (0.713‰) are presented in the Supplementary data (Table S3).

To compare our results with previous results of warm-water corals reported by Saenger et al. (2012) from the Yale laboratory, we used their results reported in the ARF (Saenger et al., 2012). These authors also shared samples with Caltech, achieving consistent results between the two labs. Therefore, the warm-water coral results in that study should also be comparable to our corrected results.

3.2.3. Clumped isotope compositions of cold-water corals

Our measured Δ_{47} values ranged from 0.797‰ to 0.875‰ for corals covering a temperature range of 2.2–17.4 °C (Tables 1 and 2, Fig. 3). We include detailed sample provenance and the temperature and seawater chemistry estimates from each different source in the Supplementary material (Table S1). Raw data of clumped isotope analyses, including all carbonate and gas standards' values, are also presented in the Supplementary material (Tables S2 and S3).

We find that, while an overall temperature dependence is observed, variations in Δ_{47} at any single temperature are greater than found by Thiagarajan et al. (2011), probably due to the larger number of individual specimens and genera analysed here. For example, the Δ_{47} of 15 corals collected from temperatures between 3 and 5 °C vary by 0.06‰, equivalent to a 12 °C range in estimated temperature using the calibration line of Ghosh et al. (2006). If data from Saenger et al. (2012) are included, this range increases to 0.08‰. This range of Δ_{47} is significantly greater than our measurement uncertainties (~0.006–0.008‰ 1 S.E. for samples with multiple replicates, Section 2.3.). In contrast, we found no significant difference in Δ_{47} (<0.02‰) between the septa and theca for any of the 7 corals studied (Table 2).

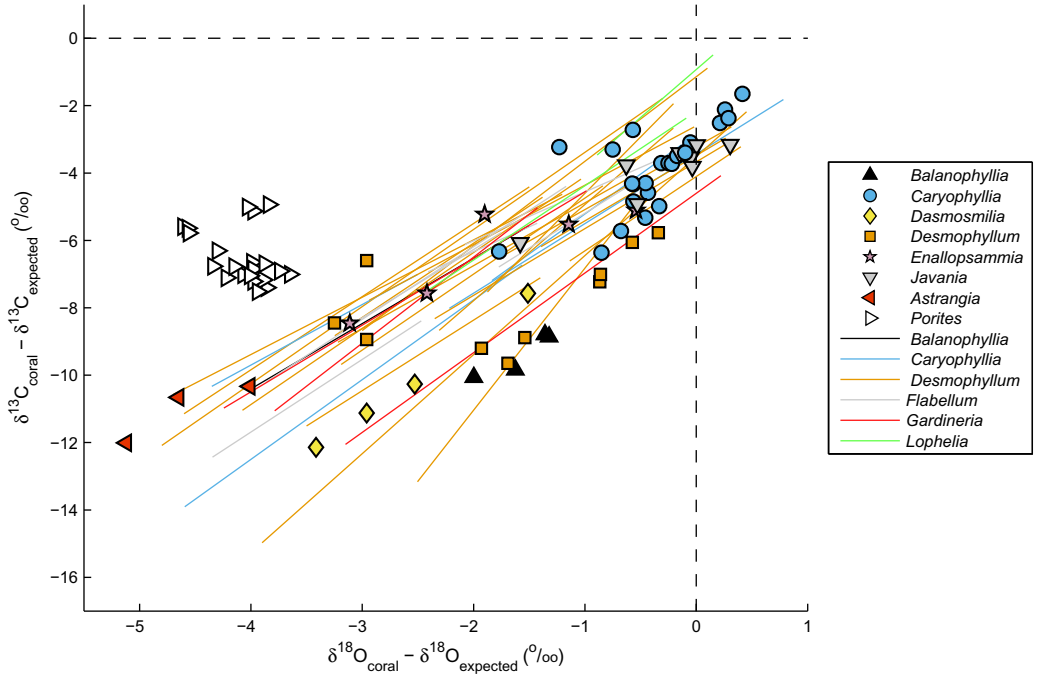

Fig. 1. Deviations of coral $\delta^{13}C$ and $\delta^{18}O$ from the expected equilibrium values. Equilibrium values were calculated based on the seawater $\delta^{13}C_{HCO_3^-}$ and $\delta^{18}O$ values determined for each sample site and the isotope fractionation factors determined by Romanek et al. (1992) (for $\delta^{13}C$) and Grossman and Ku (1986) (for $\delta^{18}O$). Shown as symbols are the bulk coral isotope measurements from this study, Thiagarajan et al. (2011) and Saenger et al. (2012). Also shown as lines are selections of data from Adkins et al. (2003) and Smith et al. (2000). Each line represents the best fit through multiple measurements on a single coral specimen, and is not extrapolated past the maximum and minimum $\delta^{18}O$ measured in the specimen. Zero offsets from the expected equilibrium for both $\delta^{13}C$ and $\delta^{18}O$ are shown as dashed black lines. For simplicity, errors bars for the stable isotope measurements are not shown in the figure, but are around ±0.6‰ 2 S.E. for $\delta^{13}C$ (based on the error in Romanek et al., 1992) and ±0.2‰ 2 S.E. for $\delta^{18}O$ for the data symbols.

4. DISCUSSION

4.1. Inter-genus variations in cold-water coral Δ_{47}

The combined coral Δ_{47} data from WHOI, Caltech and Yale highlights the previously observed first-order dependence of corals' clumped isotope compositions on their growth temperatures (Fig. 3). In accordance with previous clumped isotope studies of coral skeletal carbonates, the absolute values of our data lie more closely to the Ghosh calibration line than calibrations with shallower slopes, such as the Dennis calibration line (Fig. 3). We therefore discuss our results by reference to the Ghosh calibration line in the following sections, assuming it represents the carbonate clumped isotope equilibrium, consistent with previous clumped isotope studies of coral skeletal carbonates (Thiagarajan et al., 2011; Saenger et al., 2012).

Note: two versions of the Ghosh line have been derived in the ARF (Fig. 3. Dennis et al., 2011; Eagle et al., 2013). Although both of these were based solely on the original data reported by Ghosh et al. (2006), they are offset by ~0.01‰ due to differences in the ways in which clumped isotope measurement uncertainties were incorporated into the regression analyses. Specifically, Dennis et al. (2011) weighted their regression model based on the analytical uncertainties of each measurement, while Eagle et al. (2013) did not. In addition, Zaarur et al. (2013) recently performed additional carbonate precipitation experiments and derived a new calibration line by combining their new data with the original Ghosh et al. (2006) data. Zaarur et al. (2013) used residual-based iterative weighting to include the analytical uncertainties in their regression, resulting in a calibration line similar to that reported by Eagle et al. (2013). Although these different calibration lines lie within each other's confidence envelopes, the exact version of the calibration line we adopt may slightly alter our conclusions. Here, in the absence of a clear community agreed 'best practice', we adopt the Dennis et al. (2011) version of the Ghosh line in our following discussion, since it lies closest to the coral data.

In the absence of clumped isotope vital effects, we would expect our measured coral clumped isotope compositions to cluster evenly around the Ghosh calibration line, the assumed clumped isotope equilibrium line. In this ideal case, the offsets of measured coral Δ_{47} from the Ghosh calibration line would follow a normal distribution of mean zero, with a standard deviation equal to the long-term standard deviation for our carbonate standards representing the analytical uncertainty (Fig. 4, solid red curve). In the following analyses comparing our results to this ideal case we use only data from this study, for which all values of individual replicate measurements were available.

The distributions of offsets within each genus were indeed consistent with normal distributions, but did not have mean values of zero. Instead, with the exception of *Caryophyllia*, they tended to be offset towards higher values, with mean offsets ranging from ~0‰ to 0.04‰ (Table 5). The genera *Balanophyllia*, *Enallopsammia* and *Dasmosmilia* had higher offsets (0.03–0.04‰) than the genera *Desmophyllum*, *Caryophyllia* and *Javania* (−0.005–0.005‰).

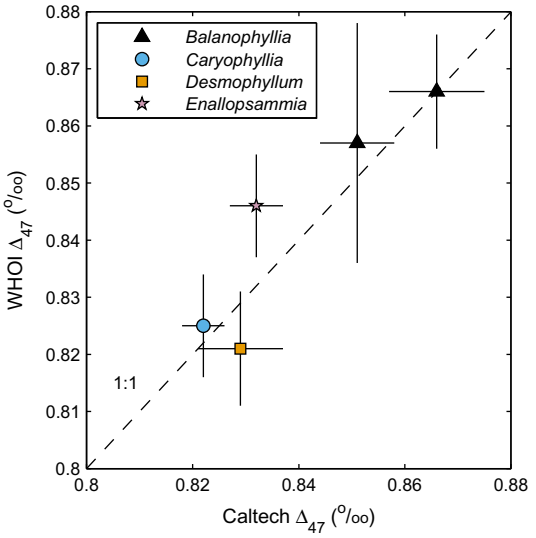

Fig. 2. Inter-laboratory comparison of clumped isotope measurements between WHOI and Caltech. Measurements were made on aliquots of the same coral powders (see Table 4). The dashed line denotes a 1:1 relationship. Errors bars are 1 S.E.

With the exception of *Caryophyllia*, chi-squared (χ^2) tests for variance suggested that the variances of the offset distributions for each genus were not distinguishable from that of multiple measurements on the carbonate standard 102-GC-AZ01 (Kanji, 2006) (Table 5). This result suggests that the spread in results for most genera can be attributed to analytical uncertainties. Samples from the genus *Caryophyllia* had a significantly greater variance than would be expected from analytical uncertainties (Table 5), which we suspect arises from the greater variety of species and morphologies sampled for this genus. Note also that, considering data from all genera, the measurement data have a broader, flatter distribution than the idealised case.

We used Kolmogorov–Smirnov (K–S) tests to evaluate the significance of the difference between the observed offset distributions for each genus and the idealised case – in this case the expected offset distribution around the Ghosh line given our measurement uncertainty (Kanji, 2006). Samples with greater numbers of replicates are likely to better reflect their true Δ_{47}. We therefore weighted the statistical analysis according to the total number of measurements on each genus, i.e. by considering each replicate measurement as an individual sample. Such a procedure means that samples with more replicates are weighted more highly. The number of measurements on any one genus ranged from 12 (for *Balanophyllia*) to 65 (for *Caryophyllia*). For the genera *Balanophyllia*, *Enallopsammia* and *Dasmosmilia*, the measured coral clumped isotope compositions did not agree with the distribution of the idealised case, instead forming distributions that were significantly offset above it (>99% likelihood of a difference, Table 5). The same results were obtained using *T*-tests, confirming that the mean offsets for each of these three genera are significantly greater than zero. It should be noted that if other versions of the

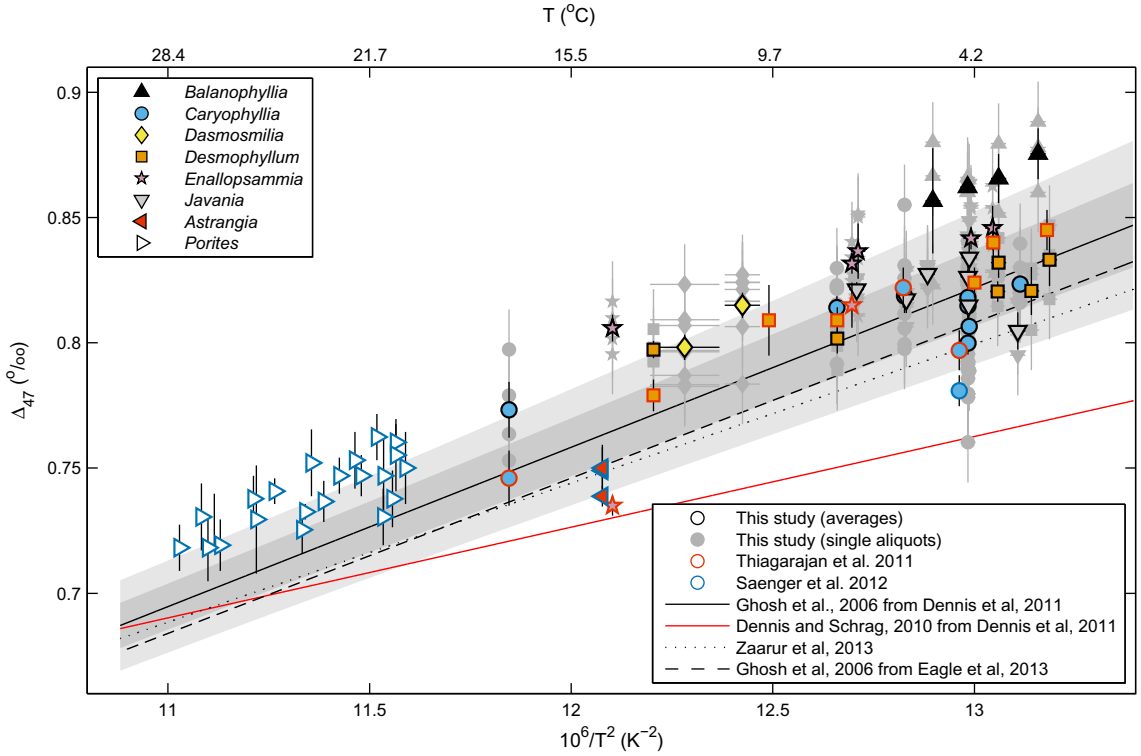

Fig. 3. Measured Δ_{47} versus temperature for corals measured during this study. Data shown are the averages of all subsamples for each coral. Also shown are cold-water and warm-water coral data from Thiagarajan et al. (2011) and Saenger et al. (2012) after conversion to the absolute reference frame (Section 2.4). In addition, the inorganic calibration lines of Ghosh et al. (2006) and Dennis and Schrag (2010) as recalculated in Dennis et al. (2011), the Ghosh line recalculated by Eagle et al. (2013) and the calibration line of Zaarur et al. (2013) are also shown. The light and dark grey envelopes represent the 2 S.E. and 1 S.E. respectively of the Ghosh line recalculated by Dennis et al. (2011). Errors bars are 1 S.E. in all cases.

inorganic Ghosh calibration are used (eg. Eagle et al., 2013; Zaarur et al., 2013), all the genera studied here have mean positive offsets that are significant according to the K–S and *T*-tests, but that the genera *Desmophyllum*, *Caryophyllia* and *Javania* remain close to the lines.

Further Kolmogorov–Smirnov tests were carried out to evaluate differences between different coral genera. These tests showed that there was no significant difference in the distributions of offsets between the genera *Desmophyllum* and *Javania*, and between *Dasmosmilia* and *Enallopsammia*. However, with the exception of these two pairs of genera, every coral genus had distributions of offsets that were significantly different to those of every other genus (Fig. 4b).

As described above, uncertainties in the Ghosh calibration line make it difficult to establish how close any particular genus lies to the inorganic equilibrium, or how large the mean offsets are for each genus. The existence of other inorganic carbonate calibration lines in the literature further complicates the interpretation of our results (Dennis and Schrag, 2010; Kim et al., 2010; Zaarur et al., 2013; Tang et al., 2014; Defliese et al., 2015; Kluge et al., 2015). For example, had we assumed that the Dennis calibration line represents the clumped isotope equilibrium, the calculated clumped isotope offsets would have been greater for all genera (e.g. ~0.1‰ for *Balanophyllia*). However, the finding that different genera have different offsets from the equilibrium values is not dependent on the assumed clumped isotope equilibrium line (Fig. S1).

Our results thus provide robust evidence of inter-genus variations in clumped isotope vital effects in cold-water corals. Inter-genus differences in clumped isotope compositions similar to those that we report here for cold-water corals have also been observed in warm-water corals. For example, the genus *Porites* was found to have Δ_{47} values systematically offset above the Ghosh calibration line, whereas the genus *Astrangia* was not (Saenger et al., 2012).

The presence of clumped isotope vital effects in certain cold-water coral genera provides further evidence that the presence or absence of symbionts is not the driver of such effects. In addition, the suggestion of Saenger et al. (2012) that corals exhibiting clumped isotope vital effects could be identified by the relationship between $\delta^{18}O$ and $\delta^{13}C$ in the skeleton does not appear to be true for cold-water corals, because all cold-water corals exhibit very similar slopes in their depletions of $\delta^{18}O$ and $\delta^{13}C$ (Fig. 1). Given our new data, it appears that the mechanism causing clumped isotope vital effects may be common to all scleractinian corals – regardless of whether they grow in cold-water or warm-water – and may act to different degrees within different genera.

Note that despite certain genera (*Balanophyllia*, *Dasmosmilia*, *Enallopsammia* and *Porites*) showing significant

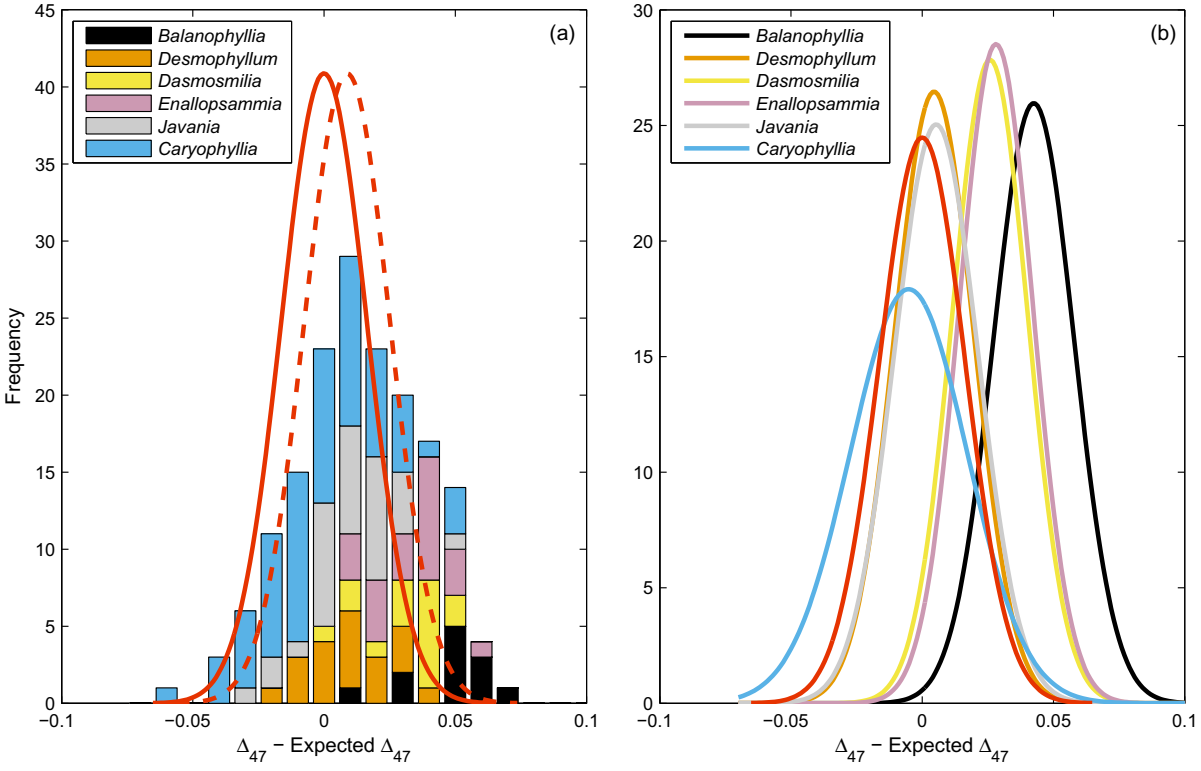

Fig. 4. Distributions of the deviations of measured coral Δ_{47} from the inorganic calibration line of Ghosh et al. (2006) recalculated by Dennis et al. (2011). (a) Stacked histogram of Δ_{47} deviations for single analyses from this study. The solid red curve represents a normal distribution centred on zero (i.e. no offset from the Ghosh calibration line) with a standard deviation equal to the long-term standard deviation of our in-house carbonate standard 102-GC-AZ01 (0.016‰). The dashed red line is the equivalent normal distribution but with a mean equal to the average offset of our coral data from the Ghosh calibration line. (b) Normalised (i.e. equal area) normal distributions for each genus of coral based on the data in (a). The red curve is the same as described for (a) but normalised. (For interpretation of the references to colour in this figure legend, the reader is referred to the web version of this article.)

clumped isotope vital effects, a relationship between Δ_{47} and temperature can still be observed within each of these genera. We suggest that with more work, species- or genus-specific temperature calibrations could be a useful approach for application of the carbonate clumped isotope thermometer in coral skeletons. However, before attempting to use such an approach, it is important to determine the causes of the observed clumped isotope vital effects. We examine possible mechanisms below, beginning with an outline of the coral calcification process that will inform further evaluations of the existing $\delta^{18}O$, $\delta^{13}C$ and Δ_{47} data.

4.2. Origins of clumped isotope vital effects in cold-water corals

4.2.1. Mechanisms of coral calcification and stable isotope vital effects

Corals are thought to precipitate carbonate from an extracellular calcifying fluid (ECF), separated from the surrounding seawater by the calicoblastic cell membrane (Fig. 5, Saenger et al., 2012). An enzymatic alkalinity pump, e.g. CaATPase, is thought to operate across the cell membrane. It removes two protons from the ECF for every

Table 5
Statistical analysis of the differences in the distributions of measured coral Δ_{47} values for each coral genus, relative to an idealised distribution around the inorganic calibration line determined by Ghosh et al. (2006). ±Values are 1 S.D. See details in Section 4.1.

Coral genus	Number of analyses	Mean offset (‰)	K–S test *p*-value	*T*-test *p*-value	χ^2 test *p*-value
Balanophyllia	12	0.042 ± 0.015	3.0×10^{-9}	1.1×10^{-6}	0.9
Enallopsammia	14	0.028 ± 0.014	1.1×10^{-8}	5.4×10^{-9}	0.4
Dasmosmilia	16	0.026 ± 0.014	5.9×10^{-7}	3.0×10^{-6}	0.6
Javania	32	0.005 ± 0.016	7.6×10^{-2}	6.9×10^{-2}	0.9
Desmophyllum	12	0.005 ± 0.015	0.36	0.20	0.7
Caryophyllia	61	-0.0051 ± 0.022	1.2×10^{-2}	6.7×10^{-2}	6.5×10^{-5}

Ca^{2+} pumped into it (Ip et al., 1991). This ionic exchange increases the pH and alkalinity of the ECF, causing DIC to speciate towards CO_3^{2-}. Accordingly the aragonite saturation state in the ECF increases, leading to enhanced aragonite precipitation. Two sources of carbon contribute to the calcification within the ECF; the $CO_{2(aq)}$ diffused across the cell membrane, and seawater DIC from seawater leakage (Fig. 5, eg. Erez, 1978; Furla et al., 2000).

Within this framework of coral calcification, several mechanisms have been proposed to explain the stable isotope ($\delta^{18}O$ and $\delta^{13}C$) vital effects observed in corals. For example, McConnaughey (1989) attributed the co-depletion of $\delta^{18}O$ and $\delta^{13}C$ in coral skeletons (Fig. 2) to kinetic isotope effects associated with CO_2 hydration/hydroxylation reactions. The kinetic isotope effects associated with these reactions can be transferred from the resulting HCO_3^- to the carbonate mineral because the rate of coral calcification (i.e. carbonate precipitation) is usually fast.

In comparison, Adkins et al. (2003) showed that the depletions of $\delta^{18}O$ and $\delta^{13}C$ in coral skeletons are actually decoupled in the dense and rapidly precipitated centres of calcification (COCs), and therefore argued that both these decoupled depletions, and the coupled depletions in the rest of the skeleton could rather be explained by changes in the pH of the ECF and the extent of CO_2 diffusion across the cell membrane. Speciation of DIC in the coral ECF varies as a function of its pH, with higher pH leading to larger fractions of CO_3^{2-} relative to HCO_3^-. Under isotope equilibrium, CO_3^{2-} has a $\delta^{18}O$ that is depleted relative to HCO_3^- (McCrea, 1950; Usdowski et al., 1991; Usdowski and Hoefs, 1993). Therefore, if coral calcification makes use of both CO_3^{2-} and HCO_3^- to form $CaCO_3$, as suggested for other carbonates (Zeebe, 1999), the higher proportion of CO_3^{2-} at high pH should lead to more depleted skeletal $\delta^{18}O$ than at lower pH (Adkins et al., 2003). Higher pH of the ECF would also promote CO_2 diffusion through the cell membrane, the depleted $\delta^{13}C$ of which would cause depleted skeletal $\delta^{13}C$. These effects could thus result in the co-variance in $\delta^{18}O$ and $\delta^{13}C$ observed in the majority of the skeleton, while allowing for the observed limit to $\delta^{13}C$ depletion in the rapidly precipitated COCs caused by a limit in the capacity for CO_2 diffusion. However, this pH-based vital effect model requires the COCs to be precipitated at the highest pH of any part of the coral, which appears to be at odds with boron isotope data (Blamart et al., 2007; Rollion-Bard et al., 2011).

4.2.2. Possible causes of observed intra- and inter-genus variations

Recent studies of coral clumped isotope compositions have examined the potential correlations between the clumped isotope and oxygen isotope variations, focusing on several key processes involved in coral calcification, e.g. diffusion, CO_2 hydration/hydroxylation and equilibrium isotope fractionation amongst different DIC species (Guo et al., 2009a; Thiagarajan et al., 2011; Saenger et al., 2012; Tripati et al., 2015). Guo et al. (2009a) made first-order estimates about the effects of CO_2 hydration/hydroxylation reactions on the carbonate clumped isotope composition and suggested that they could result in negative slopes of $\Delta(\Delta_{47})/\Delta(\delta^{18}O)$ on the order of −0.05 to −0.01 respectively, where $\Delta(\Delta_{47}) = \Delta_{47}–\Delta_{47(eq)}$ and $\Delta(\delta^{18}O) = \delta^{18}O–\delta^{18}O_{(eq)}$ are defined as the deviations of the coral clumped isotope and oxygen isotope compositions from their expected equilibrium values. An estimate for the effect of CO_2 diffusion through the lipid-bilayer (based on Knudson diffusion) predicted a similar slope of −0.023 (Thiagarajan et al., 2011), although this diffusion model predicts smaller than observed depletions in $\delta^{13}C$ for a unit depletion in $\delta^{18}O$ (Thiagarajan et al., 2011; Saenger et al., 2012). Importantly, both of the above processes apply only to DIC derived from the CO_2 diffused across the cell membrane and not to DIC from the leaked seawater (ambient DIC). In the absence of other processes, pH-driven changes in the ratio of CO_3^{2-} to HCO_3^- in the ECF, and thus that incorporated into the skeleton, are not thought to have a large effect on the resulting Δ_{47}, because the difference in the $^{13}C–^{18}O$ clumping effects between these species is quite small; $(\Delta_{63_{HCO_3^-}})–(\Delta_{63_{CO_{32}^-}}) = 0.018‰$ (Guo et al., 2008) or 0.033‰ (Hill et al., 2014) at ~300 K. Calculating the effect of changing pH results in a positive $\Delta(\Delta_{47})/\Delta(\delta^{18}O)$ slope of ~0.002 (Guo et al., 2009a; Thiagarajan et al., 2011; Saenger et al., 2012), ~0.004 if the $(\Delta_{63_{HCO_3^-}})–(\Delta_{63_{CO_{32}^-}})$ value from Hill et al. (2014) is used, and up to ~0.01 based on experimental data (Guo et al., 2012; Tripati et al., 2015). We refer to the pH effect modelled in Hill et al. (2014) for the remainder of the study, noting that it represents an intermediate estimate of the impact of pH change on carbonate Δ_{47}.

We compare our coral isotope data with these preliminary theoretically predicted $\Delta(\Delta_{47})/\Delta(\delta^{18}O)$ slopes to determine the likely processes governing the clumped isotope vital effects in scleractinian corals. Again we assume that the Ghosh calibration line, as recalculated in Dennis et al. (2011), represents the carbonate clumped isotope equilibrium in the following discussion. Our broad conclusions are not affected by this choice of calibration line, but we acknowledge that our detailed interpretations may change should a different calibration line prove more realistic (e.g. Figs. S2, S3).

As described above (Section 3.2.), the intra-coral variation of $\delta^{18}O$ and Δ_{47}, e.g. septa vs. theca, are small in all the coral specimens examined (<1.5‰ for $\delta^{18}O$, <0.02‰ for Δ_{47} respectively). This result suggests that the Δ_{47} ranges observed amongst our corals are not simply related to differences between these two macroscopic skeletal architectures. The coral JC094-B0468-Daslm-001 (*Dasmosmilia* sp.) showed the maximum difference in $\delta^{18}O$ between the septa and theca, and was associated with a positive $\Delta(\Delta_{47})/\Delta(\delta^{18}O)$ slope of 0.006 ± 0.016. This slope is very similar to the slope predicted for pH-driven isotope fractionation (0.002–0.01), although both septal and thecal Δ_{47} were offset significantly above the expected equilibrium values (by ~0.016–0.026‰), lying at least partially within the region predicted for kinetic effects associated with CO_2 hydration and hydroxylation reactions (Fig. 6a). Given estimated slopes of −0.05, −0.01 and −0.02 for the CO_2 hydration and CO_2 hydroxylation reactions and diffusive processes respectively, and the uncertainties on the

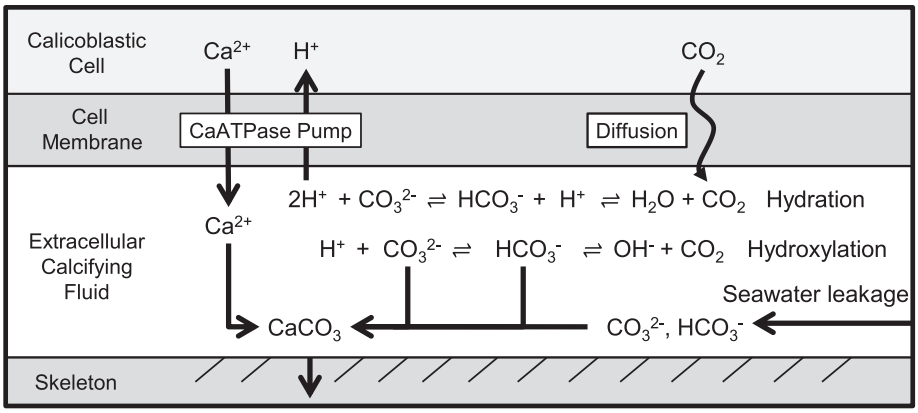

Fig. 5. Schematic diagram of coral calcification, modified after Saenger et al. (2012). Labels and equations indicate the processes involved during coral calcification. Descriptions of each process are given in the text.

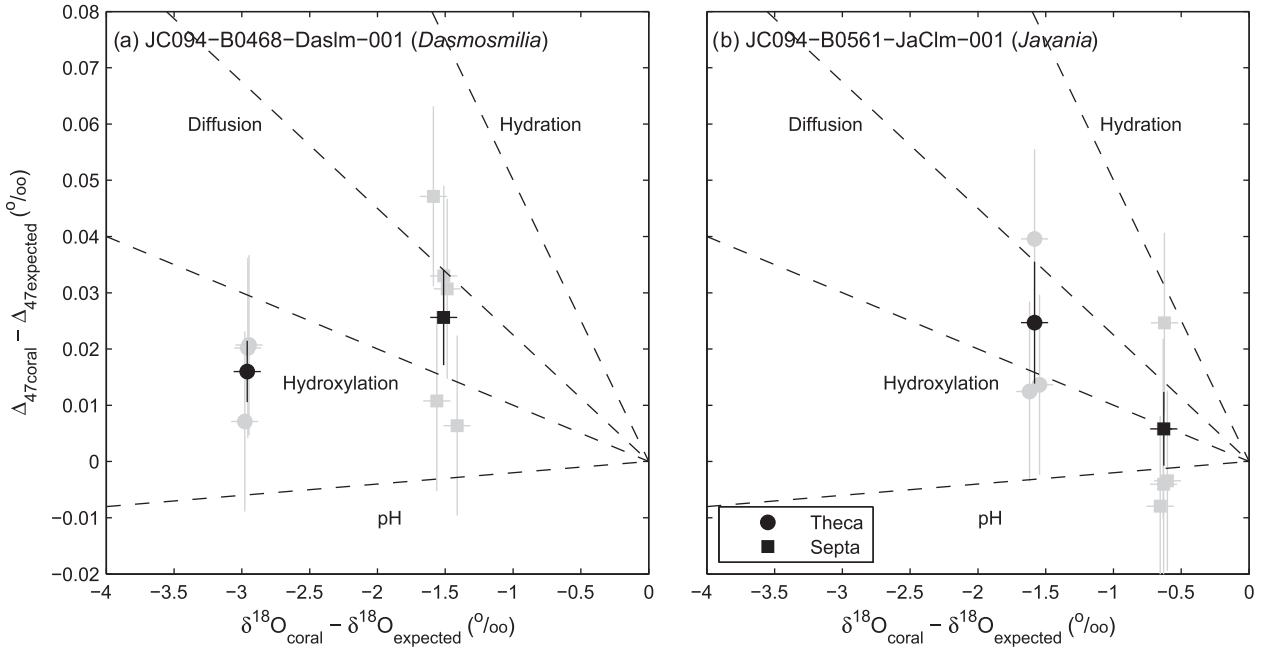

Fig. 6. Intra-coral variations of the measured Δ_{47} and $\delta^{18}O$ and their deviations from the expected equilibrium values. Examples are shown for two corals: (a) JC094-B0468-Daslm-001 (*Dasmosmilia*) and (b) JC094-B0561-JaClm-001 (*Javania*), where samples were taken from both the theca and septa. Faded and solid symbols represent individual measurements and averages of replicate measurements respectively. The expected equilibrium values are calculated using the equations in Ghosh et al. (2006) – recalculated by Dennis et al. (2011) – and Grossman and Ku (1986) respectively. Dashed lines show the modelled trajectories of hydration/hydroxylation kinetic effects, diffusive effects and equilibrium precipitation at varying pH (Section 4.2.2). Error bars are 1 S.E.

observed theca-septa $\Delta(\Delta_{47})/\Delta(\delta^{18}O)$ slope, this sample suggests that the more extreme slopes predicted for kinetic effects may not explain the intra-coral variation here. However, the large uncertainties on the slope do not preclude less extreme kinetic isotope effects (i.e. CO_2 hydroxylation) acting within this sample. The sample JC094-B0561-Jav-001 (*Javania*) also had a relatively large difference in $\delta^{18}O$ between the septa and theca (0.9‰). In this case the slope between the two data points was negative (-0.020 ± 0.024), very similar to the slope for diffusional effects and lying within the region bound by the slopes of the CO_2 hydration and hydroxylation reactions (Fig. 6b). However, the large uncertainties do not rule out a slope equal to that of a pH-driven vital effect. Therefore, our isotope measurements within single specimens cannot isolate one mechanism causing intra-coral isotope vital effects at the macro-scale. Further detailed work could aim to investigate intra-coral variation further, including the impacts of micro-scale features, such as centres of calcification.

The greater range in $\delta^{18}O$ within and between different coral genera allows us to evaluate the mechanisms of observed vital effects further. We plot isotope data for those

genera that exhibit $\delta^{18}O$ depletions large enough to establish relationships between $\Delta(\Delta_{47})$ and $\Delta(\delta^{18}O)$ in Fig. 7a, and plot data for the other genera separately in Fig. 7b. In general, warm-water corals appear to exhibit a larger depletion in $\delta^{18}O$ than cold-water corals despite similar ranges in $\Delta(\Delta_{47})$. All genera appear to be consistent with near-zero slopes of $\Delta(\Delta_{47})/\Delta(\delta^{18}O)$, but as previously highlighted, different genera have different offsets from the expected Δ_{47} equilibrium, suggesting differences in the vital effect mechanisms between them. For example, a line of best fit through the *Desmophyllum* data (WHOI and Caltech) has a slope of -0.0013 ± 0.0024 and an intercept of 0.0066 ± 0.0045, suggesting variations in the pH of the ECF are a primary control on the variability of $\delta^{18}O$ and

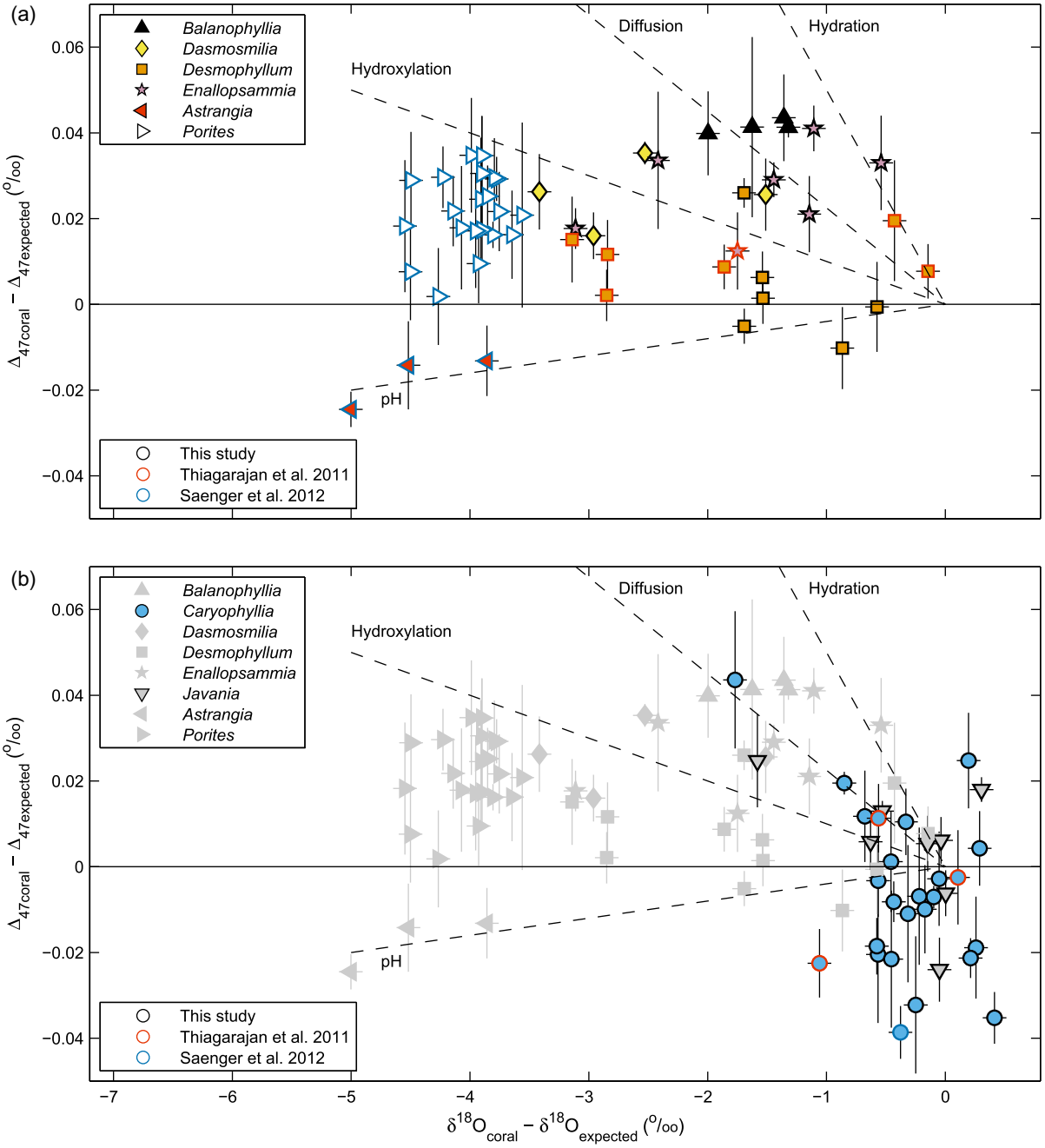

Fig. 7. Deviations of the measured coral Δ_{47} and $\delta^{18}O$ from the expected equilibrium values for different coral genera. (a) Subsample (i.e. theca or septa) averages for coral genera with >1‰ depletions in $\delta^{18}O$. (b) Subsample (i.e. theca or septa) averages for coral genera with <1‰ depletions in $\delta^{18}O$; other genera are shown as faded symbols. Also shown are cold-water and warm-water coral data from Thiagarajan et al. (2011) and Saenger et al. (2012) after conversion to the absolute reference frame (Section 2.4). The expected equilibrium values are calculated using the equations in Ghosh et al. (2006) – recalculated by Dennis et al. (2011) – and Grossman and Ku (1986) respectively. Dashed lines show the modelled trajectories of hydration/hydroxylation kinetic effects, diffusive effects and equilibrium precipitation at varying pH (Section 4.2.2). Error bars are 1 S.E.

Δ_{47} amongst the different individuals of this genus. The warm-water genus *Astrangia* could also be consistent with this pattern. However, given the uncertainties associated with the Ghosh line described previously, it is possible that the Δ_{47} of the genus *Desmophyllum* may also be systematically above the clumped isotope equilibrium (Figs. S2, S3). Better constraints on the inorganic equilibrium line will be needed to fully address this question.

The cold-water genera *Balanophyllia*, *Dasmosmilia* and *Enallopsammia* seem to be inconsistent with pH being the sole driver of isotope variations, lying in the region broadly covered by the first-order models of the effects of CO_2 hydration/hydroxylation and/or diffusion (Fig. 7a). This observation is also true for the two data points for the genera *Caryophyllia* and *Javania* that have $\delta^{18}O$ depletions of >1‰ (Fig. 7b). The warm-water genus *Porites* exhibits similar Δ_{47} offsets to the cold-water corals in Fig. 7a, ranging from ~0–0.04‰, suggesting that a similar range of Δ_{47} vital effects could be in operation for both groups of corals. As noted above, the diffusion model predicts smaller than observed depletions in $\delta^{13}C$ per unit depletion in $\delta^{18}O$ (Thiagarajan et al., 2011; Saenger et al., 2012). Therefore, kinetic effects associated with CO_2 hydration/hydroxylation reactions would appear to be the more likely candidate for causing the clumped isotope vital effects observed for these samples.

Of course, it is likely that multiple processes act in concert during coral calcification and simultaneously affect the isotope composition of coral skeleton, producing the whole range of isotope signatures observed, including the genus-specific differences observed here. If true, this may complicate the comparison between the experimental data and the model predicted $\Delta(\Delta_{47})/\Delta(\delta^{18}O)$ slopes for each individual process acting independently. Future modelling work should aim to systematically take into account the effects of multiple processes in order to more accurately constrain the role of each process in determining the isotope composition of coral skeletons, and to test whether species- or genus-specific calibration of clumped isotope thermometers would be appropriate.

5. CONCLUSIONS

We have tested the calibration of the carbonate clumped isotope thermometer in cold-water scleractinian corals, using a new set of samples that includes six of coral genera. We validated our clumped isotope data by directly comparing measurements made in two different laboratories (WHOI and Caltech) on the same sample powders. We found excellent agreement between laboratories once the data were normalised with reference to the in-house carbonate standards, suggesting that this normalisation may be a useful way to remove inter-laboratory biases which were not removed by converting clumped isotope data into the absolute reference frame.

We show that some cold-water coral genera exhibit clumped isotope vital effects, with their Δ_{47} values consistently higher than the expected equilibrium values, similar to findings for some warm-water corals (Saenger et al., 2012). The similarity between cold-water and warm-water corals with respect to the ranges of clumped isotope vital effects observed supports previous suggestions that the presence or absence of symbiotic algae is not a governing factor for clumped isotope vital effects in scleractinian corals. Instead, we suggest that these vital effects are most likely related to kinetic effects associated with CO_2 hydration/hydroxylation reactions within the extracellular calcifying fluid of the corals and are common to both warm- and cold-water corals. We found no significant difference in Δ_{47} between the theca and septa of individual specimens, suggesting that macro-scale skeletal features are not related to variations in Δ_{47}. Current uncertainty in the appropriate clumped isotope equilibrium line complicates the detailed interpretations of our results. However, the fact that the magnitudes of the clumped isotope offsets from expected equilibrium vary between different coral genera is not dependent on the choice of clumped isotope equilibrium line, and suggests that clumped isotope vital effects are present and expressed more in some genera than others. Further research into the differences between different inorganic calibration lines will be important in determining the presence and causes of clumped isotope vital effects in any given coral genus.

Our data complicate the use of the carbonate clumped isotope thermometer in corals, suggesting that it cannot be straightforwardly applied across all species of cold-water coral without introducing significant uncertainty into reconstructed temperatures. However, given the apparent temperature dependence of Δ_{47}, even in genera exhibiting significant clumped isotope vital effects, we suggest that the use of species-specific calibrations could still be a useful approach. In order to determine the reliability of this thermometer back through time, further work should also test it in fossil samples by comparison with other, independent temperature proxies, such as the Li/Mg ratio in corals (Case et al., 2010; Hathorne et al., 2013; Raddatz et al., 2013; Montagna et al., 2014).

ACKNOWLEDGEMENTS

We thank Prof. Benjamin H. Passey for generously providing the 102-GC-AZ01 carbonate standard and help during the construction of the automated clumped isotope analysis system at WHOI and Professors John Eiler and Jess Adkins for providing the facilities at Caltech for the inter-laboratory comparison study and for helpful discussion. This work was supported by a British National Environment Research Council studentship to P. Spooner (NE/K500823/1), National Science Foundation Grant NSF-ANT-1246387 and The Penzance Endowed Fund in Support of Assistant Scientists (WHOI) to W. Guo, and by funds from the European Research Council, the Leverhulme Trust and a Marie Curie Reintegration grant. Oxygen isotope analyses of seawater samples at BGS were funded by the NERC Isotope Geosciences Facilities Steering Committee.

APPENDIX A. SUPPLEMENTARY DATA

Supplementary data associated with this article can be found, in the online version, at http://dx.doi.org/10.1016/j.gca.2016.01.023.

REFERENCES

Adkins J. F., Boyle E. A., Curry W. B. and Lutringer A. (2003) Stable isotopes in deep-sea corals and a new mechanism for "vital effects". *Geochim. Cosmochim. Acta* **67**, 1129–1143.

Alibert C. and McCulloch M. T. (1997) Strontium/calcium ratios in modern Porites corals from the Great Barrier Reef as a proxy for sea surface temperature: calibration of the thermometer and monitoring of ENSO. *Paleoceanography* **12**, 345–363.

Barker S., Cacho I., Benway H. and Tachikawa K. (2005) Planktonic foraminiferal Mg/Ca as a proxy for past oceanic temperatures: a methodological overview and data compilation for the Last Glacial Maximum. *Quat. Sci. Rev.* **24**, 821–834.

Blamart D., Rollion-Bard C., Meibom A., Cuif J. P., Juillet-Leclerc A. and Dauphin Y. (2007) Correlation of boron isotopic composition with ultrastructure in the deep-sea coral Lophelia pertusa: implications for biomineralization and paleo-pH. *Geochem. Geophys. Geosyst.* **8**, Q12001.

Burke A. and Robinson L. F. (2012) The Southern Ocean' role in carbon exchange during the last deglaciation. *Science* **335**, 557–561.

Burke A., Robinson L. F., McNichol A. P., Jenkins W. J., Scanlon K. M. and Gerlach D. S. (2010) Reconnaissance dating: a new radiocarbon method applied to assessing the temporal distribution of Southern Ocean deep-sea corals. *Deep-Sea Res. Part I-Oceanogr. Res. Pap.* **57**, 1510–1520.

Cairns S. D. (2007) Deep-water corals: an overview with special reference to diversity and distribution of deep-water Scleractinian corals. *Bull. Mar. Sci.* **81**, 311–322.

Came R. E., Eiler J. M., Veizer J., Azmy K., Brand U. and Weidman C. R. (2007) Coupling of surface temperatures and atmospheric CO_2 concentrations during the Palaeozoic era. *Nature* **449**, 198–201.

Came R. E., Brand U. and Affek H. P. (2014) Clumped isotope signatures in modern brachiopod carbonate. *Chem. Geol.* **377**, 20–30.

Case D. H., Robinson L. F., Auro M. E. and Gagnon A. C. (2010) Environmental and biological controls on Mg and Li in deep-sea scleractinian corals. *EPSL* **300**, 215–225.

Cheng H., Adkins J., Edwards R. L. and Boyle E. A. (2000) U–Th dating of deep-sea corals. *Geochim. Cosmochim. Acta* **64**, 2401–2416.

Defliese W. F., Hren M. T. and Lohmann K. C. (2015) Compositional and temperature effects of phosphoric acid fractionation on Δ_{47} analysis and implications for discrepant calibrations. *Chem. Geol.* **396**, 51–60.

Dennis K. J. and Schrag D. P. (2010) Clumped isotope thermometry of carbonatites as an indicator of diagenetic alteration. *Geochim. Cosmochim. Acta* **74**, 4110–4122.

Dennis K. J., Affek H. P., Passey B. H., Schrag D. P. and Eiler J. M. (2011) Defining an absolute reference frame for 'clumped' isotope studies of CO_2. *Geochim. Cosmochim. Acta* **75**, 7117–7131.

Eagle R. A., Eiler J. M., Tripati A. K., Ries J. B., Freitas P. S., Hiebenthal C., Wanamaker, Jr., A. D., Taviani M., Elliot M., Marenssi S., Nakamura K., Ramirez P. and Roy K. (2013) The influence of temperature and seawater carbonate saturation state on C-13–O-18 bond ordering in bivalve mollusks. *Biogeosciences* **10**, 4591–4606.

Eiler J. M. and Schauble E. (2004) (OCO)-O-18-C-13-O-16 in Earth's atmosphere. *Geochim. Cosmochim. Acta* **68**, 4767–4777.

Erez J. (1978) Vital effect on stable-isotope composition seen in foraminifera and coral skeletons. *Nature* **273**, 199–202.

Falkowski P. G., Dubinsky Z., Muscatine L. and Porter J. W. (1984) Light and the bioenergetics of a symbiotic coral. *Bioscience* **34**, 705–709.

Furla P., Galgani I., Durand I. and Allemand D. (2000) Sources and mechanisms of inorganic carbon transport for coral calcification and photosynthesis. *J. Exp. Biol.* **203**, 3445–3457.

Gagnon A. C., Adkins J. F., Fernandez D. P. and Robinson L. F. (2007) Sr/Ca and Mg/Ca vital effects correlated with skeletal architecture in a scleractinian deep-sea coral and the role of Rayleigh fractionation. *EPSL* **261**, 280–295.

Gao P., Xu X., Zhou L., Pack M. A., Griffin S., Santos G. M., Southon J. R. and Liu K. (2014) Rapid sample preparation of dissolved inorganic carbon in natural waters using a headspace-extraction approach for radiocarbon analysis by accelerator mass spectrometry. *Limnol. Oceanogr.* **12**, 174–190.

Ghosh P., Adkins J., Affek H., Balta B., Guo W. F., Schauble E. A., Schrag D. and Eller J. M. (2006) (13)C–(18)O bonds in carbonate minerals: a new kind of paleothermometer. *Geochim. Cosmochim. Acta* **70**, 1439–1456.

Grossman E. L. and Ku T. L. (1986) Oxygen and carbon isotopic fractionation in biogenic aragonite – temperature effects. *Chem. Geol.* **59**, 59–74.

Guo W., Daeron M., Niles P., Genty D., Kim S. T., Vonhof H., Affek H., Wainer K., Blamart D. and Eiler J. (2008) C-13–O-18 bonds in dissolved inorganic carbon: implications for carbonate clumped isotope thermometry. *Geochim. Cosmochim. Acta* **72**. A336.

Guo W., Kim S., Thiagarajan N., Adkins J. F. and Eiler J. M. (2009) Mechanisms for "vital effects" in biogenic carbonates: new perspectives based on abundances of 13C–18O bonds. Eos Trans. AGU 90, Fall Meet. Suppl. PP34B-07 (abstr.).

Guo W., Mosenfelder J. L., Goddard, III, W. A. and Eiler J. M. (2009b) Isotopic fractionations associated with phosphoric acid digestion of carbonate minerals: insights from first-principles theoretical modeling and clumped isotope measurements. *Geochim. Cosmochim. Acta* **73**, 7203–7225.

Guo W., Kim S. T., Yuan J. and Farquhar J. B. P. (2012) 13C–18O bonds in dissolved inorganic carbon: toward a better understanding of clumped isotope thermometer in biogenic carbonates. *Mineral. Mag.* **76**, 1791.

Hathorne E. C., Felis T., Suzuki A., Kawahata H. and Cabioch G. (2013) Lithium in the aragonite skeletons of massive Porites corals: A new tool to reconstruct tropical sea surface temperatures. *Paleoceanography* **28**, 143–152.

Henkes G. A., Passey B. H., Wanamaker, Jr., A. D., Grossman E. L., Ambrose, Jr., W. G. and Carroll M. L. (2013) Carbonate clumped isotope compositions of modern marine mollusk and brachiopod shells. *Geochim. Cosmochim. Acta* **106**, 307–325.

Hill P. S., Tripati A. K. and Schauble E. A. (2014) Theoretical constraints on the effects of pH, salinity, and temperature on clumped isotope signatures of dissolved inorganic carbon species and precipitating carbonate minerals. *Geochim. Cosmochim. Acta* **125**, 610–652.

Huntington K. W., Eiler J. M., Affek H. P., Guo W., Bonifacie M., Yeung L. Y., Thiagarajan N., Passey B., Tripati A., Daeron M. and Came R. (2009) Methods and limitations of 'clumped' CO_2 isotope (Delta(47)) analysis by gas-source isotope ratio mass spectrometry. *J. Mass Spectr.* **44**, 1318–1329.

Ip Y. K., Lim A. L. L. and Lim R. W. L. (1991) Some properties of calcium-activated adenosine-triphosphate from the hermatypic coral *Galxea-fascicularis*. *Mar. Biol.* **111**, 191–197.

Kanji G. K. (2006) *100 Statistical Tests*, 3 ed. SAGE Publications Ltd.

Kim S. T., Guo W., Coplen T. B., Farquhar J. and Eiler J. M. (2010) Temperature dependence of C-13–O-18 clumping in synthetic aragonite: laboratory calibration. *Geochim. Cosmochim. Acta* **74**. A517-A517.

Kluge T., John C. M., Jourdan A. L., Davis S. and Crawshaw J. (2015) Laboratory calibration of the calcium carbonate

clumped isotope thermometer in the 25–250 °C temperature range. *Geochim. Cosmochim. Acta* **157**, 213–227.

Levitus S., Boyer T. P. (1994) World Ocean Atlas 1994 Volume 4: Temperature, number 4.

Lopez Correa M., Montagna P., Vendrell-Simon B., McCulloch M. and Taviani M. (2010) Stable isotopes (delta O-18 and delta C-13), trace and minor element compositions of recent scleractinians and Last Glacial bivalves at the Santa Maria di Leuca deep-water coral province, Ionian Sea. *Deep-Sea Res. Part Ii-Topical Stud. Oceanogr.* **57**, 471–486.

Lutringer A., Blamart D., Frank N. and Labeyrie L. (2005) Paleotemperatures from deep-sea corals: scale effects. In *2nd International Symposium on Deep-Sea Corals, Erlangen, Germany*. pp. 1081–1096.

Marali S., Wisshak M., Lopez Correa M. and Freiwald A. (2013) Skeletal microstructure and stable isotope signature of three bathyal solitary cold-water corals from the Azores. *Palaeogeogr. Palaeoclimatol. Palaeoecol.* **373**, 25–38.

Margolin A., Robinson L. F., Burke A., Waller R. G., Scanlon K. M., Roberts M. L., Auro M. E. and van de Flierdt T. (2014) Temporal and spatial distributions of cold-water corals in the Drake Passage: insights from the last 35,000 years. *Deep Sea Res. Part II: Topical Stud. Oceanogr.* **99**, 237–248.

McConnaughey T. (1989) ^{13}C and ^{18}O isotopic disequilibrium in biological carbonates. 1. Patterns. *Geochim. Cosmochim. Acta* **53**, 151–162.

McCrea J. M. (1950) On the isotopic chemistry of carbonates and a paleotemperature scale. *J. Chem. Phys.* **18**, 849–857.

Montagna P., McCulloch M., Douville E., Lopez Correa M., Trotter J., Rodolfo-Metalpa R., Dissard D., Ferrier-Pages C., Frank N., Freiwald A., Goldstein S., Mazzoli C., Reynaud S., Ruggeberg A., Russo S. and Taviani M. (2014) Li/Mg systematics in scleractinian corals: calibration of the thermometer. *Geochim. Cosmochim. Acta* **132**, 288–310.

Mook W. G., Bommerso J. C. and Staverma W. H. (1974) Carbon isotope fractionation between dissolved bicarbonate and gaseous carbon-dioxide. *EPSL* **22**, 169–176.

Mortensen P. B. and Rapp H. T. (1998) Oxygen and carbon isotope ratios related to growth line patterns in skeletons of *Lophelia pertusa* (L.) (Anthozoa, Scleractinia): implications for determination of linear extension rates. *Sarsia* **83**, 433–446.

Petrizzo D. A., Young E. D. and Runnegar B. N. (2014) Implications of high-precision measurements of C-13–O-18 bond ordering in CO_2 for thermometry in modern bivalved mollusc shells. *Geochim. Cosmochim. Acta* **142**, 400–410.

Porter J. W., Muscatine L., Dubinsky Z. and Falkowski P. G. (1984) Primary production and photoadaptation in light-adapted and shade-adapted colonies of the sybiotic coral, *Stylophora-pistillata*. *Proc. R. Soc. Lond. B-Biol. Sci.* **222**, 161–180.

Raddatz J., Liebetrau V., Rueggeberg A., Hathorne E., Krabbenhoeft A., Eisenhauer A., Boehm F., Vollstaedt H., Fietzke J., Lopez Correa M., Freiwald A. and Dullo W. C. (2013) Stable Sr-isotope, Sr/Ca, Mg/Ca, Li/Ca and Mg/Li ratios in the scleractinian cold-water coral Lophelia pertusa. *Chem. Geol.* **352**, 143–152.

Roberts J. M. and Cairns S. D. (2014) Cold-water corals in a changing ocean. *Curr. Opin. Environ. Sustain.* **7**, 118–126.

Roberts J. M., Wheeler A. J. and Freiwald A. (2006) Reefs of the deep: the biology and geology of cold-water coral ecosystems. *Science* **312**, 543–547.

Roberts J. M., Wheeler A. J., Freiwald A. and Cairns S. D. (2009) *Cold-Water Corals: The Biology and Geology of Deep-Sea Coral Habitats*. Cambridge University Press, 368 p.

Robinson L.F. (2014) RRS James Cook Cruise JC094, October 13–November 30 2013, Tenerife-Trinidad. TROPICS, Tracing Oceanic Processes using Corals and Sediments. Reconstructing abrupt changes in chemistry and circulation of the equatorial Atlantic Ocean: implications for global climate and deep-water habitats.

Robinson L. F., Adkins J. F., Frank N., Gagnon A. C., Prouty N. G., Roark E. B. and van de Flierdt T. (2014) The geochemistry of deep-sea coral skeletons: a review of vital effects and applications for palaeoceanography. *Deep-Sea Res. Part II-Topical Stud. Oceanogr.* **99**, 184–198.

Rollion-Bard C., Blamart D., Cuif J. P. and Juillet-Leclerc A. (2003) Microanalysis of C and O isotopes of azooxanthellate and zooxanthellate corals by ion microprobe. *Coral Reefs* **22**, 405–415.

Rollion-Bard C., Blamart D., Cuif J.-P. and Dauphin Y. (2010) In situ measurements of oxygen isotopic composition in deep-sea coral, *Lophelia pertusa*: re-examination of the current geochemical models of biomineralization. *Geochim. Cosmochim. Acta* **74**, 1338–1349.

Rollion-Bard C., Blamart D., Trebosc J., Tricot G., Mussi A. and Cuif J.-P. (2011) Boron isotopes as pH proxy: a new look at boron speciation in deep-sea corals using B-11 MAS NMR and EELS. *Geochim. Cosmochim. Acta* **75**, 1003–1012.

Romanek C. S., Grossman E. L. and Morse J. W. (1992) Carbon isotopic fractionation in synthetic aragonite and calcite – effects of temperature and precipitation rate. *Geochim. Cosmochim. Acta* **56**, 419–430.

Rosenheim B. E., Tang J. and Fernandez A. (2013) Measurement of multiply substituted isotopologues ('clumped isotopes') of CO_2 using a 5 kV compact isotope ratio mass spectrometer: performance, reference frame, and carbonate paleothermometry. *Rapid Commun. Mass Spectrom.* **27**, 1847–1857.

Rueggeberg A., Fietzke J., Liebetrau V., Eisenhauer A., Dullo W.-C. and Freiwald A. (2008) Stable strontium isotopes (delta Sr-88/86) in cold-water corals – a new proxy for reconstruction of intermediate ocean water temperatures. *EPSL* **269**, 569–574.

Saenger C., Affek H. P., Felis T., Thiagarajan N., Lough J. M. and Holcomb M. (2012) Carbonate clumped isotope variability in shallow water corals: temperature dependence and growth-related vital effects. *Geochim. Cosmochim. Acta* **99**, 224–242.

Schmidt G. A., Bigg G. R. and Rohling E.J. (1999) Global Seawater Oxygen-18 Database – v1.21. http://data.giss.nasa.gov/o18data/.

Smith J. E., Schwarcz H. P., Risk M. J., McConnaughey T. A. and Keller N. (2000) Paleotemperatures from deep-sea corals: overcoming 'vital effects'. *Palaios* **15**, 25–32.

Spiro B., Roberts M., Gage J. and Chenery S. (2000) O-18/O-16 and C-13/C-12 in an ahermatypic deepwater coral *Lophelia pertusa* from the North Atlantic: a case of disequilibrium isotope fractionation. *Rapid Commun. Mass Spectrom.* **14**, 1332–1336.

Stanley G. D. J. and Cairns S. D. (1988) Constructional azooxanthellate coral communities: an overview with implications for the fossil record. *Palaios* **3**, 233–242.

Tang J., Dietzel M., Fernandez A., Tripati A. K. and Rosenheim B. E. (2014) Evaluation of kinetic effects on clumped isotope fractionation (Delta(47)) during inorganic calcite precipitation. *Geochim. Cosmochim. Acta* **134**, 120–136.

Thiagarajan N., Adkins J. and Eiler J. (2011) Carbonate clumped isotope thermometry of deep-sea corals and implications for vital effects. *Geochim. Cosmochim. Acta* **75**, 4416–4425.

Thiagarajan N., Subhas A. V., Southon J. R., Eiler J. M. and Adkins J. F. (2014) Abrupt pre-Bolling-Allerod warming and circulation changes in the deep ocean. *Nature* **511**, 75–78.

Tripati A. K., Eagle R. A., Thiagarajan N., Gagnon A. C., Bauch H., Halloran P. R. and Eiler J. M. (2010) C-13–O-18 isotope

signatures and 'clumped isotope' thermometry in foraminifera and coccoliths. *Geochim. Cosmochim. Acta* **74**, 5697–5717.

Tripati A. K., Hill P. S., Eagle R. A., Mosenfelder J. L., Tang J., Schauble E. A., Eiler J. M., Zeebe R. E., Uchikawa J., Coplen T. B., Ries J. B. and Henry D. (2015) Beyond temperature: clumped isotope signatures in dissolved inorganic carbon species and the influence of solution chemistry on carbonate mineral composition. *Geochim. Cosmochim. Acta* **166**, 344–371.

Usdowski E. and Hoefs J. (1993) Oxygen-isotope exchange between carbonic-acid, bicarbonate, carbonate, and water – a reexamination of the data of McCrea (1950) and an expression for the overall partitioning of oxygen isotopes between the carbonate species and water. *Geochim. Cosmochim. Acta* **57**, 3815–3818.

Usdowski E., Michaelis J., Bottcher M. E. and Hoefs J. (1991) Factors for the oxygen isotope equilibrium fractionation between aqueous and gaseous CO_2, carbonic acid, bicarbonate, carbonate and water (19-degrees-C). *J. Phys. Chem. Chem. Phys.* **170**, 237–249.

van Heuven S., Pierrot D., Rae J. W. B., Lewis E. and Wallace D. W. R. (2011) *MATLAB program developed for CO_2 system calculations. ORNL/CDIAC-105b*. Carbon Dioxide Information Analysis Centre, Oak Ridge National Laboratory, U.S. Department of Energy, Oak Ridge, Tennessee.

Zaarur S., Olack G. and Affek H. P. (2011) Paleo-environmental implication of clumped isotopes in land snail shells. *Geochim. Cosmochim. Acta* **75**, 6859–6869.

Zaarur S., Affek H. P. and Brandon M. T. (2013) A revised calibration of the clumped isotope thermometer. *EPSL* **382**, 47–57.

Zeebe R. E. (1999) An explanation of the effect of seawater carbonate concentration on foraminiferal oxygen isotopes. *Geochim. Cosmochim. Acta* **63**, 2001–2007.

Associate editor: Claire Rollion-Bard